



# Simuleringsstudie ved bruk av "HeaveLock" for dempning av nedhullssvingninger som følge av hivbevegelser i rig

**Monica Sandell**

Master i kybernetikk og robotikk

Innlevert: januar 2016

Hovedveileder: Ole Morten Aamo, ITK

Norges teknisk-naturvitenskapelige universitet  
Institutt for teknisk kybernetikk



---

# Problem description

## Background

In drilling operations performed in the oil and gas industry it is important to control pressure of the drilling fluid, also called drilling mud. Drilling mud is used primarily for removing cuttings from the well. It is injected at high pressure at the top of the drill string. At the end of the drill string, called the drilling bit, the drilling mud flows into the annulus and then rises together with cuttings up to the surface. At the surface, the cuttings are separated from the mud and the cleaned mud is re-injected into the drill string for further circulation. Apart from removing cuttings from the well, drilling mud is also needed for pressurizing the well. If the pressure in the well is too low hydrocarbons can flow into the well and potentially develop into a blowout. If the pressure exceeds a certain threshold, it may fracture the well leading to loss of mud into the formation. For this reason, it is important to control mud pressure in the well.

In managed pressure drilling (MPD) operations, the well is sealed at the top and the pressure is controlled by opening/closing the valve that releases the mud at the top of the well. This technology has proven successful when drilling from stationary platforms. When drilling from a floater, however, the heaving motion of the floater causes major pressure fluctuations in the well, which must be compensated for using automatic control. Several studies have been performed in the search for a remedy for the problem, all considering main pump shutdown during connections. The objective of this project is to investigate the effect of continuous circulation and the use of "HeaveLock" on the pressure oscillations. In order to do so, some revision of our models is needed in addition to carrying out the simulations study. The following points should be addressed by the student:

## Problem statement

1. Review prior work on the heave-problem, and in particular work on modeling.
2. Model: review the capabilities of the simulator and suggest any necessary modifications.
3. Perform a simulation study that demonstrates the capabilities of the Heave-Lock under various conditions (well depth, heave height, pump rate etc.). Suggest a complete procedure for a connection with HeaveLock, starting from drilling ahead - shutting down the heave-compensation system, 10 minute

---

connection, turning on heave-compensation, back to drilling ahead. How should the HeaveLock behave during these steps, and can it do it autonomously?

4. Write a report.

**Start date:** 2015-09-07

**Due date:** 2016-02-01

**Thesis performed at:** Department of Engineering Cybernetics, NTNU

**Supervisor:** Professor Ole Morten Aamo, Dept. of Eng. Cybernetics, NTNU

---

# Summary

Easily obtained oil is today already produced. New and mature fields do exist, but many opportunities are situated in conditions, making them hard to drill. As there is also a recession in oil price due to the current political situation of the world (Guardian, 2015), this is also an incentive to increase profitability of fields.

When drilling in challenging conditions, Managed Pressure Drilling (MPD) techniques can be used to avoid pressure related difficulties. One such difficulty is when a floating rig needs to make a connection, ie. extend its pipe. When this is done, the pipe is fastened to the oil rig, and the rig movements can no longer be decoupled from the pipe movements, making conventional MPD techniques unusable. Heave motion of the rig makes the drillstring act as a piston in the well, with surge and swab, creating both high and low pressures. The strategy today is to wait for weather conditions to be at a satisfactory level, and resume operation.

The HeaveLock project aims to solve this problem. The HeaveLock actuator is a valve mounted inside the drillstring, above the bit, regulating the downhole pressure oscillations due to the surge and swab motions.

This thesis is a simulation study of the HeaveLock in an oil well. The most vital parameters in the simulator for the function of the HeaveLock in making connections are identified. A connection procedure is found, with a satisfactory regulation of the downhole pressure oscillations, however all improvements of the procedure come at a cost. A smaller nominal HeaveLock opening demands a higher pump pressure and creates pressure disturbance at initialization and termination of the HeaveLock. Time intervals can be lengthened and create better terms in disturbances, but as it is desired to make a connection as effective as possible, this is also considered a downside.

A connection is however documented, showing the best possible configuration found in this study. For the active period of the HeaveLock, about 70% of the downhole pressure oscillations can be dampened, with disturbances of 3.2 bar and 3.7 bar due to the termination of the HeaveLock.

---

---

# Sammendrag

Lett anskaffet olje er i dag allerede produsert. Både nye og modne felt med muligheter finnes, men mange ligger i forhold som gjør dem vanskelig å bore. Det er også en lavere oljepris enn det har vært i lang tid, som resultat av den nåværende verdenssituasjonen (Guardian, 2015), og dette også et insentiv til å øke lønnsomheten i felt.

Ved boring i krevende forhold, kan Managed Pressure Drilling (MPD-teknikker) brukes for å unngå trykkrelaterte problemer. Et slikt problem er for eksempel når en flytende rigg må gjøre en forlengelse, altså å forlenge borestrengen. Da blir strengen festet til oljeriggen og eventuell hivbevegelse i riggen gjør at borestrengen fungerer som et stempel i brønnen, og skaper både høye og lave trykk. Riggbevegelser kan da ikke lenger frikoples matematisk fra strengens bevegelser, noe som gjør at konvensjonelle MPD-teknikker ikke kan brukes. Strategien i dag er å vente til at vær og vind er på et tilfredsstillende nivå, for og så gjenoppta driften.

HeaveLockprosjektet er et forsøk på å løse dette problemet. HeaveLockaktuatoren er en ventil montert inne i borestrengen, over bitet, med formålet å regulere trykksvingninger i brønnen, spesielt nedihull.

Denne avhandlingen er en simuleringstudie av HeaveLock i en oljebrønn. De viktigste parameterne i simulatoren, for funksjonen av HeaveLock når den skal gjøre en forlengelse, er identifisert. En prosedyre for fremgangsmåte er funnet, med en tilfredsstillende regulering av nedihulls trykksvingninger. Alle endringer av parametre som forbedrer prosedyren har derimot sin pris. En mindre nominell HeaveLock åpning krever et høyere pumpetrykk og skaper trykkforstyrrelse ved initialisering og terminering av HeaveLock. Tidsintervaller kan forlenges og skape bedre vilkår i forstyrrelser, men ettersom det er ønskelig å gjøre forlengelsen så effektiv som mulig, blir dette også sett som en ulempe.

En forlengelsesprosedyre er imidlertid dokumentert, og viser best mulig konfigurasjon som er funnet i denne avhandlingen. For den aktive perioden av HeaveLock, så kan rundt 70% av nedihulls trykksvingninger dempes, med 3,2 bar og 3,7 bar i nedrampingsforstyrrelse.

---

---

# Preface

This document is the authors master thesis at the Department of Engineering Cybernetics at the Norwegian University of Science and Technology, NTNU, and was written in the time period from September 2015 until January 2016.

Readers are assumed to have a higher education in a technical field, with basic understanding of modeling, physics and fluid mechanics. No understanding of Managed Pressure Drilling (MPD) specifically is required, but would be an advantage in understanding the motivation behind the assignment.

I would like to thank Ole Morten Aamo for being my advisor, and for guiding me through the semester. Furthermore, a thank you to Anders Dahlen for valuable feedback and inspiration, helping me with all of my questions on code and otherwise. Thanks is also owed to Timm Strecker for taking the time to answer my coding questions. At last I would like to thank my fellow students for making my time at NTNU unforgettable.

---

---

# Contents

---

|   |            |
|---|------------|
| <b>Problem formulation</b>                      | <b>i</b>   |
| <b>Summary</b>                                  | <b>i</b>   |
| <b>Sammendrag</b>                               | <b>i</b>   |
| <b>Preface</b>                                  | <b>iii</b> |
| <b>Table of Contents</b>                        | <b>vi</b>  |
| <b>List of Tables</b>                           | <b>vii</b> |
| <b>List of Figures</b>                          | <b>x</b>   |
| <b>Abbreviations</b>                            | <b>xi</b>  |
| <b>Glossary</b>                                 | <b>xi</b>  |
| <b>Notations</b>                                | <b>xii</b> |
| <b>1 Introduction</b>                           | <b>1</b>   |
| 1.1 Motivation . . . . .                        | 1          |
| 1.2 Previous work . . . . .                     | 2          |
| 1.2.1 Background of the IPT Heave Lab . . . . . | 2          |
| 1.3 Outline of thesis . . . . .                 | 3          |
| <b>2 Background on drilling and MPC</b>         | <b>5</b>   |
| 2.1 Conventional drilling . . . . .             | 5          |

---

|             |  |           |
|-------------|--|-----------|
| 2.1.1       | Formations and discovery . . . . .                     | 6         |
| 2.1.2       | Mud system . . . . .                                   | 6         |
| 2.1.3       | Blowout . . . . .                                      | 7         |
| 2.2         | Managed Pressure Drilling (MPD) . . . . .              | 7         |
| 2.2.1       | Continuous circulation . . . . .                       | 8         |
| 2.2.2       | The Heave Attenuation problem . . . . .                | 8         |
| <b>3</b>    | <b>Real Plant Simulator</b>                            | <b>11</b> |
| 3.1         | The hydraulic well model . . . . .                     | 11        |
| 3.1.1       | Discretization . . . . .                               | 13        |
| 3.1.2       | Modeling the downhole section . . . . .                | 14        |
| 3.2         | The HeaveLock model . . . . .                          | 16        |
| 3.2.1       | HeaveLock control . . . . .                            | 17        |
| <b>4</b>    | <b>HeaveLock connection</b>                            | <b>19</b> |
| 4.1         | Simulation environment . . . . .                       | 19        |
| 4.2         | Conditions for making a connection . . . . .           | 20        |
| 4.3         | Initialization example . . . . .                       | 21        |
| 4.4         | A successful connection . . . . .                      | 22        |
| <b>5</b>    | <b>Well Dimentions Effect on Simulations - Results</b> | <b>25</b> |
| 5.1         | Nominal Heave Lock opening . . . . .                   | 25        |
| 5.2         | Well depth . . . . .                                   | 28        |
| 5.3         | Flow rate . . . . .                                    | 31        |
| <b>6</b>    | <b>Connection simulations - Results</b>                | <b>37</b> |
| 6.1         | Connection simulation example . . . . .                | 37        |
| 6.2         | HeaveLock ramping time . . . . .                       | 38        |
| 6.3         | HeaveLock build up time . . . . .                      | 44        |
| 6.4         | Summary of time parameters . . . . .                   | 47        |
| 6.5         | A tighter simulation . . . . .                         | 49        |
| 6.6         | A Short connection . . . . .                           | 52        |
| <b>7</b>    | <b>Discussion</b>                                      | <b>55</b> |
| <b>8</b>    | <b>Conclusion</b>                                      | <b>57</b> |
| 8.1         | Further work . . . . .                                 | 58        |
|             | <b>Bibliography</b>                                    | <b>59</b> |
|             | <b>Appendix</b>  | <b>61</b> |
| Appendix A: | The RealPlant Simulator . . . . .                      | 61        |

---

---

## List of Tables

---

|     |   |    |
|-----|---|----|
| 4.1 | Time parameters which have to be defined for simulations. . . . . | 21 |
| 4.2 | Time parameters defined for example in Section 4.3. . . . .       | 22 |
| 6.1 | Time parameters defined for example in Section 6.1. . . . .       | 40 |

---

---

## List of Figures

---

|      |  |    |
|------|--|----|
| 1.1  | The new setup of the IPT Heave Lab. . . . .  | 3  |
| 2.1  | Setup of an offshore drilling system. . . . .  | 9  |
| 3.1  | Downhole model. . . . .  | 14 |
| 3.2  | Mechanical design of the HeaveLock valve. . . . .  | 16 |
| 4.1  | HeaveLock opening, flow rate and choke opening of an exemplified simulation. . . . .       | 23 |
| 4.2  | Downhole pressure of an exemplified simulation. . . . .                                    | 24 |
| 5.1  | Case 1a, $u_0 = 0.15$ . . . . .  | 26 |
| 5.2  | Case 1b, $u_0 = 0.3$ . . . . .   | 27 |
| 5.3  | Case 1c, $u_0 = 0.5$ . . . . .   | 28 |
| 5.4  | Case 2a, $L = 1000$ m. . . . .   | 29 |
| 5.5  | Case 2b, $L = 4000$ m. . . . .   | 30 |
| 5.6  | Case 2c, $L = 10000$ m. . . . .  | 31 |
| 5.7  | Case 2a, b and c, $v_{BHA}$ . . . . .  | 32 |
| 5.8  | Case 3a, $q = 600 \frac{1}{\text{min}}$ . . . . .  | 33 |
| 5.9  | Case 3b, $q = 1500 \frac{1}{\text{min}}$ . . . . .   | 34 |
| 5.10 | Case 3c, $q = 3000 \frac{1}{\text{min}}$ . . . . .   | 35 |
| 6.1  | Connection example case, downhole pressure . . . . .                                       | 38 |
| 6.2  | Connection example case, inputs . . . . .  | 39 |
| 6.3  | Case 4a, $\Delta t_{hl}^1 = \Delta t_{hl}^2 = 20$ s, HeaveLock opening. . . . .            | 41 |
| 6.4  | Case 4a, $\Delta t_{hl}^1 = \Delta t_{hl}^2 = 20$ s, downhole pressure difference. . . . . | 41 |
| 6.5  | Case 4b, $\Delta t_{hl}^1 = \Delta t_{hl}^2 = 100$ s, HeaveLock opening. . . . .           | 42 |

---

|      |   |    |
|------|---|----|
| 6.6  | Case 4b, $\Delta t_{hl}^1 = \Delta t_{hl}^2 = 100$ s, downhole pressure difference. . . . . | 43 |
| 6.7  | Case 4c, $\Delta t_{hl}^1 = \Delta t_{hl}^2 = 150$ s, HeaveLock opening. . . . .            | 43 |
| 6.8  | Case 4c, $\Delta t_{hl}^1 = \Delta t_{hl}^2 = 150$ s, downhole pressure difference. . . . . | 44 |
| 6.9  | Case 5a, $t_{hl}^{buildup} = 30$ s, HeaveLock opening. . . . .                              | 45 |
| 6.10 | Case 5a, $t_{hl}^{buildup} = 30$ s, downhole pressure difference. . . . .                   | 46 |
| 6.11 | Case 5b, $t_{hl}^{buildup} = 100$ s, HeaveLock opening. . . . .                             | 46 |
| 6.12 | Case 5b, $t_{hl}^{buildup} = 100$ s, downhole pressure difference. . . . .                  | 47 |
| 6.13 | Case 5c, $t_{hl}^{buildup} = 200$ s, HeaveLock opening. . . . .                             | 48 |
| 6.14 | Case 5c, $t_{hl}^{buildup} = 200$ s, downhole pressure difference. . . . .                  | 48 |
| 6.15 | Case 6, summary of time simulations. HeaveLock opening. . . . .                             | 50 |
| 6.16 | Case 6, summary of time simulations. Downhole pressure difference. . . . .                  | 50 |
| 6.17 | Case 7, lowering $u_0$ for a connection. HeaveLock opening and pump<br>pressure. . . . .    | 51 |
| 6.18 | Case 7, lowering $u_0$ for a connection. Downhole pressure difference. . . . .              | 52 |
| 6.19 | Case 8, 2.5 min connection, HeaveLock opening. . . . .                                      | 53 |
| 6.20 | Case 8, 2.5 min connection,, downhole pressure difference. . . . .                          | 53 |

---

# Abbreviations

|      |   |   |
|------|---|---|
| BHA  | = | Bottom hole assembly                                  |
| CBHP | = | Constant bottomhole pressure                          |
| CCS  | = | Continuous circulation system                         |
| IADC | = | The International Association of Drilling Contractors |
| IPT  | = | Department of Petroleum Engineering                   |
| MPD  | = | Managed Pressure Drilling                             |
| NPT  | = | Non-Productive Time                                   |
| NTNU | = | Norwegian University of Science and Technology        |
| ODE  | = | Ordinary Differential Equation                        |
| PDE  | = | Partial Differential Equation                         |

# Oil & Gas Glossary

|                      |   |  |
|----------------------|---|--|
| Annulus              | = | The void between the piping or drillstring, and the walls surrounding it                           |
| Back pressure        | = | Pressure in the drillstring  |
| Ballast tank         | = | Compartment on a boat of a platform which uses ballast to provide stability or weight for a vessel |
| Bit                  | = | Tool used to crush rock at the bottom of the drillstring   |
| Blowout              | = | Uncontrolled flow of formation fluids from a well  |
| Bottom hole assembly | = | The lower part of the drillstring  |
| Conduit              | = | A channel for conveying fluid  |
| Cuttings             | = | Small pieces of rock that break away due to the bit  |
| Downhole             | = | Lower part of the oil well, below the bit  |
| Drillstring          | = | Combination of drillpipe, BHA and other tools used to make the bit                                 |
| Floater              | = | Floating oil rig   |
| Formation fluid      | = | Fluids occurring in the pores of a rock  |
| Kick                 | = | Flow of formation fluids into the well during drilling operations                                  |
| Mud                  | = | Drilling fluid   |
| Topside              | = | At rig level of operation  |
| Wellbore             | = | The drilled hole   |

Most descriptions are reported from Schlumberger (2016).

---

# Notations

|             |   |  |
|-------------|---|--|
| $A_a$       | = | Cross-section area of annulus                  |
| $A_{BHA}$   | = | Cross-section area of BHA                      |
| $A_{bit}$   | = | Cross-section area of bit                      |
| $A_i$       | = | Cross-section area inside pipe                 |
| $A_p$       | = | Cross-section area of pipe                     |
| $\beta$     | = | Bulk modulus                                   |
| $\beta_a$   | = | Bulk modulus of annulus                        |
| $\beta_i$   | = | Bulk modulus in pipe                           |
| $d_{BHA}$   | = | Diameter of BHA                                |
| $E$         | = | Young modulus of pipe                          |
| $F_a$       | = | Annulus nonlinear friction term                |
| $f_a$       | = | hoop-stress coefficient of annulus             |
| $F_i$       | = | Nonlinear friction term in pipe                |
| $f_i$       | = | hoop-stress coefficient of inside of pipe      |
| $F_\rho$    | = | Friction term of pipe walls                    |
| $F_v$       | = | Friction term due to pressure drop through BHA |
| $g$         | = | Acceleration due to gravity                    |
| $K_c$       | = | Topside choke characteristic                   |
| $k_{hl}$    | = | HeaveLock choke characteristic                 |
| $L$         | = | Well debth                                     |
| $p_a$       | = | Pressure in annulus                            |
| $p_a tm$    | = | Atmospheric pressure                           |
| $p_{hl}$    | = | HeaveLock pressure                             |
| $p_i$       | = | Pressure inside pipe                           |
| $\rho$      | = | Density  |
| $\rho_{dh}$ | = | Density of downhole section                    |
| $q_a$       | = | Flow in annulus                                |
| $q_{bit}$   | = | Flow through bit                               |
| $q_{des}$   | = | Desired flow through HeaveLock                 |
| $q_{hl}$    | = | Flow through HeaveLock                         |
| $q_i$       | = | Flow in pipe                                   |
| $q_p$       | = | Pump flow                                      |
| $q_r$       | = | Flow around BHA                                |
| $t$         | = | Time   |
| $\theta_a$  | = | Annulus angle                                  |
| $\theta_i$  | = | Inside of pipe angle                           |
| $\theta_p$  | = | Pipe angle                                     |
| $u$         | = | Choke opening                                  |
| $u_0$       | = | Nominal HeaveLock opening                      |
| $u_{hl}$    | = | HeaveLock opening                              |
| $v_{BHA}$   | = | Velocity of BHA                                |
| $V_{dh}$    | = | Volume of downhole section                     |
| $V_{hole}$  | = | Control volume of hole                         |

---

$v_p$  = Velocity of pipe  
 $v_{rig}$  = Velocity of rig  
 $x$  = Vertical movement of the BHA

## Subscripts

$a$  = annulus  
 $BHA$  = bottom hole assembly  
 $i$  = in pipe  
 $p$  = pipe  
 $r$  = out of the BHA

---

# CHAPTER 1

---

## Introduction

---

### 1.1 Motivation

In many reservoirs there remains potential; readily available prospects are already tapped while other opportunities may require a very narrow pressure window to stay within. Surpassing this window in either direction may cause disastrous results, both economically and environmentally.

In drilling from stationary platforms, a simple manual opening and closing of a valve at the top of the well can be sufficient in controlling the pressure fluctuations in the *downhole* section. However, when drilling from a *floater*, pressure fluctuations due to heave motion of the rig have to be compensated for using automated control. This type of control method is categorized as *Managed Pressure Drilling* (MPD). Existing MPD already exist for ahead drilling, but when the *drillstring* is extended, it is connected to the rig, and the movements of the drillstring can no longer be decoupled from the rig movement. The approach used in drilling operations today is to wait for weather conditions to settle, to resume operation.

Compensating for these pressure changes would increase the safety and the timeliness of drilling operations while yielding financial reward, if no shut-down is required. The goal of this thesis is to simulate the HeaveLock actuator to investigate whether it has the potential to enable exploration of difficult prospects.

---

## 1.2 Previous work

Previously, the heave attenuation problem has been tackled in a number of ways. Godhavn et al. (2011) and Øyvind Breyholtz et al. (2009) present MPD methods used in attenuation from stationary platforms. (Kaasa, 2000) investigated a single control volume, and Kaasa et al. (2010) used the same model, but here for faster dynamics, proving that this type of model is not sufficient for other than very slow system dynamics.

Landet (2011) developed an advanced hydraulic transmission line model for advanced control, and discovered previously used models were insufficient. It does not, however, consider how the *mud* in the drillstring effects the pipe velocity, which Mitchell (1988) documents.

In Aarsnes (2012), the well is described as a hydraulic transmission line and linearized by using a Laplace transform, and Kalman filter estimated the downhole pressure. Albert et al. (2014) tackled the heave attenuation problem by using a sealed well with a *topside* choke and a backpressure pump to control pressure. The work of this thesis is a continuation of the work done then, with an alteration in the form of a new actuator. Schaut (2015) describes a hydraulic model, which is used in the simulator of this thesis, and therefore rendered in later chapters along with the modeling of the HeaveLock actuator.

### 1.2.1 Background of the IPT Heave Lab

In 2013, a heave lab was installed at the Department of Petroleum Engineering (IPT) and Applied Geophysics at NTNU. The lab was a research project sponsored by Statoil, using a choke at the top of the well to control downhole pressure oscillations. The work is documented in Albert (2013) and Albert et al. (2014). The lab identified a model, and a controller was developed for the choke and demonstrated in the lab. However, the control method of using a topside choke was later proved too slow to handle the well dynamics.

Later the HeaveLock device was suggested. In late 2015, the IPT-Heave Lab has been rebuilt as in Figure 1.1. The new lab, constructed by the IPT and ITK faculties at NTNU will be used to test the HeaveLock in a constructed environment.

### The RealPlant Simulator

The simulator, Real Plant, used in this thesis, was scripted by a Ph.D. student at NTNU, Timm Strecker, partly based on the hydraulic model in Aarsnes (2012). This previous version of Real Plant was without the Heave Lock functionality.

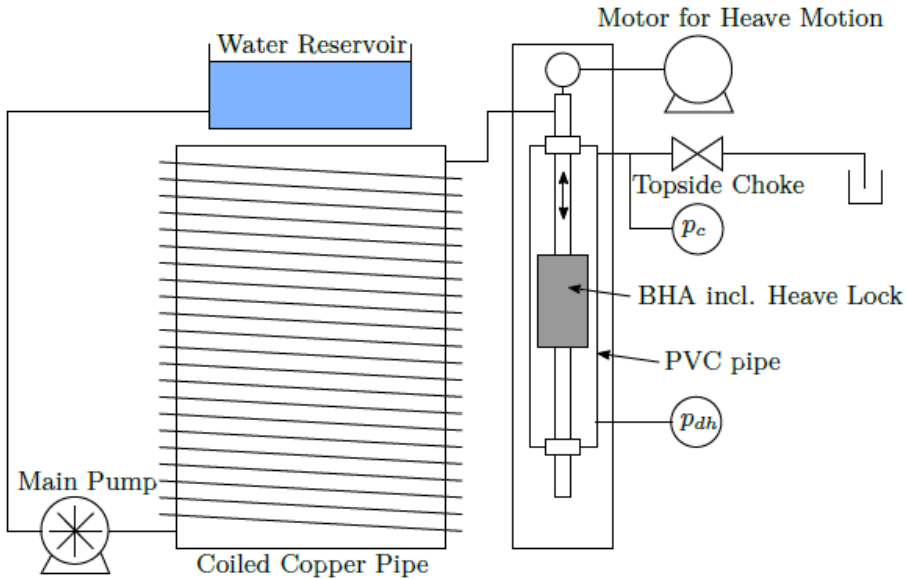


**Figure 1.1:** The new setup of the IPT Heave Lab. The figure is extracted from Schaut (2015).

In Schaut (2015), the Heave Locks solenoids are identified, suggesting a control procedure for the IPT Heave Lab. This identification was used to implement a HeaveLock into the RealPlant simulator, and also to make a HeaveLab simulator. Control solutions for the RealPlant, suggested in Schaut (2015) were not successful, however, the knowledge was used to construct a new control of the HeaveLock, which is presented in Section 3.2.

These simulators are a part of the project trying to realize the use of the HeaveLock in the real world, by using them as a safe and cheap way to foresee real world problems.

## 1.3 Outline of thesis

This thesis is divided into four main parts, the first part, chapters 1 and 2 provide background on the heave attenuation problem, some previous work done to resolve attenuation problems and background on conventional heave attenuation used outside of connections.

The second part of the thesis, chapters 3 and 4 can be considered the theory part. Chapter 3 explains the basis of the RealPlant simulator, the modeling of the well and the HeaveLock. Chapter 4 introduces conditions needed, and what is required to make a successful connection.

Chapters 5 and 6 contain the results of this thesis. While the cases simulated in Chapter 5 investigate well dimensioning effect on the HeaveLocks performance, Chapter 6 presents cases simulating connections. The latter chapter demonstrates altering of the parameters found to have the greatest effect on the performance of the connection.

Finally, chapters 7 and 8, the discussion and conclusion chapters, discuss the results found, suggest issues possible to investigate in the future and make a conclusion of the work made in this thesis.

## CHAPTER 2

---

### Background on drilling and MPC

---

Well control is exerted to minimize loss of oil, for both of environmental and economic reasons. Usually, the focus of well control is to keep kicks from happening. A *kick* is what happens when *formation fluids* enter the *annulus*, as a result of the pressure of the weight of the column of drilling fluid not being big enough to repress the formation fluids weight.

A worst case scenario of a kick could be a *blowout*. Blowout preventers (BOP's) are a specialized mechanical device used to control a well, preventing it from a blowout. BOP's are a required mechanism in oil rigs, but they do have limitations; a maximum pressure rating is not sufficient in many drilling cases.

### 2.1 Conventional drilling

In oil and gas offshore drilling, there exist two main types of platforms; fixed or floating. Fixed platforms are only used while producing an oil field; these are permanently mounted on the seabed and are dismantled or demolished when the field is produced. In addition to drill production wells, injection wells are also drilled to inject water or gas in order to increase production.

Floating platforms are movable, generally constructed from steel, and are used both for discovering new fields, drilling new wells and for production. During drilling, the platform is usually lowered by using ballast tanks, to make the platform more

stable. An alternative is to have sinkable poles that can be propped up against the seabed, but this is only possible in shallow waters (Birkeland, 2009).

In conventional drilling, the well pressure is controlled by the pumping of mud down the drillstring. When wanting to alter the well pressure, the only option for this system is to change the mud density or to change the rate at which the mud is being pumped. These changes are made manually by an operator. If the well pressure is too small, and there is an influx in the downhole section, the system is closed, and a valve is closed to reach a pressure that is high enough to resume operation. As the control of a conventional drilling system lies with the operator, it is prone to human error and potential inexperience of the operator.

### 2.1.1 Formations and discovery

When searching for a well, geologists try to locate the conditions necessary for oil entrapment. Surface rocks, terrain, and satellite images are some of the factors considered in the analysis. Other methods used could also be a detection of changes in the earth's gravity field, indicating moving oil, or changes in the earth's magnetic field, again indicating oil in motion.

Seismology is another important detection mechanism. Sound waves made using an air gun, a vibrator or dynamite, can be sent from near the sea surface, and travel through layers of rock and sand, and bounce back as echoes. Geologists can use this by analyzing the echoes, creating a seismic picture of what is beneath the seabed (International Association of Geophysical Contractors, 2014).

The seismic survey helps the petroleum geologists decide whether the conditions are present for there to be oil and gas beneath the surface. If they are, an exploration well is drilled, and if these results are confirming the seismic result, more geologists are brought on to performed more detailed seismic surveys and to drill more exploration wells. Eventually, platforms and pipelines are designed for the field.

### 2.1.2 Mud system

Mud is a product of oil, water, and chemicals, composed according to the properties needed for the drilling process. The composition of the drilling fluid is demanding, because of environmental and safety needs. The following list describes the uses of mud in drilling

- Stabilization of well pressure by increasing well pressure to maintain pressure on walls of the well
- Adding buoyancy, reducing the stress on the well due to the weight of the drillstring
- Keeping *cuttings* from building up and blocking the well

- Stabilization of rocks, keeping the mud from being absorbed by surrounding rocks
- Lubrication of equipment
- Delivering hydraulic energy, keeping fluids in the well moving
- Reducing friction, and thereby heat from contact with the rock formation

The mud is pumped into the well from the platform, down the drillstring, through the wellhead, and returns to the topside through the annulus. On the platform, the mud is recycled and returned.

### 2.1.3 Blowout

In well drilling subsea, excess pressures or low pressures can arise from surrounding rock formations, where gas or fluids from formation pockets can leak into the well, causing a blowout. In most cases, this starts with a kick; when the drilling mud cannot compensate for the increased well pressure. A blowout can also be caused by loss of drilling mud into the well formation, giving a loss of the continuous circulation, and there is a resulting pressure loss, which again can lead to a kick in the form of a well collapse. A worst-case scenario of this is a blowout, with fluids blowing out of the well, potentially damaging drilling equipment and the platform.

## 2.2 Managed Pressure Drilling (MPD)

MPD is a term of the automatic methods for drilling in challenging environments while controlling the well pressure in a sufficient manner. This is done using equipment to control the pressure of a sealed well and gives an accurate way of controlling the amount of fluids that are produced.

The aim of MPD techniques is to keep well pressure controlled, above the pore pressure. However, when using simple MPC surveillance of pressure transmitters, it does not always provide sufficient control. Especially in difficult conditions like gas pockets in the formation, weather conditions, etc., existing methods may not provide sufficient attenuation. The more the MPC technique used can handle its environment, the less Non-Productive Time (NPT), increasing the overall cost effectiveness of a given well.

Reported from Birkeland (2009), the term MPD is defined by The International Association of Drilling Contractors (IADC) defined MPD as (IADC, 2008):

- *"MPD is an adaptive drilling process used to precisely control the annular pressure profile throughout the wellbore. The objectives are to ascertain the downhole pressure environment limits and to manage the annular hydraulic pressure profile accordingly. It is the intention of MPD to avoid a continuous*

*influx of formation fluids to the surface. Any influx incidental to the operation will be safely contained using an appropriate process.*

- *MPD process employs a collection of tools and techniques which may mitigate the risks and costs associated with drilling wells that have narrow downhole environmental limits, by proactively managing the annular hydraulic pressure profile.*
- *MPD may include control of back pressure, fluid density, fluid rheology, annular fluid level, circulating friction, hole geometry or combinations thereof*
- *MPD may allow a faster corrective action to deal with observed pressure variations. The ability to dynamically control annular pressures facilitates drilling of what might otherwise be economically unattainable prospects.”*

Constant bottomhole pressure (CBHP) is an MPD technique, which seals the well, and controls the flow out of the well by a choke at the annulus exit, and a pump, giving a faster way to control the bottomhole pressure than changing the mud weight (Albert et al., 2014).

Although advanced MPD techniques exist, some will require great computing power in for example predicting disturbances, and research is still in need to find viable solutions for extreme conditions.

### **2.2.1 Continuous circulation**

Continuous circulation systems (CCS) is a technology allowing the drill pipe to be extended while having continuous flow through the well. In comparison to conventional drilling, when making a connection, the well is usually shut down until the completion of the connection and the drilling can be resumed.

CCS give advantages, as stopping the circulation of mud through the well, gives zero flow and could cause an increase in pressure due to an inflow of formation fluids (Jenner et al., 2005). CCS eliminates some negative, and positive pressure surges when making a connection, due to the eliminated need of shut-down, and eliminates the time used after a conventional connection to circulate cuttings out of a well in addition to many other problems associated with shut-down and start-up.

The CCS is a foundation for the work done in this thesis; it suggests a complete connection procedure, for which CCS is assumed.

### **2.2.2 The Heave Attenuation problem**

During a normal drilling operation, the motion of the floating rig can be decoupled from the drill strings movements, and heave motion is compensated for using conventional MPC techniques. When the drill string needs to be extended, it has

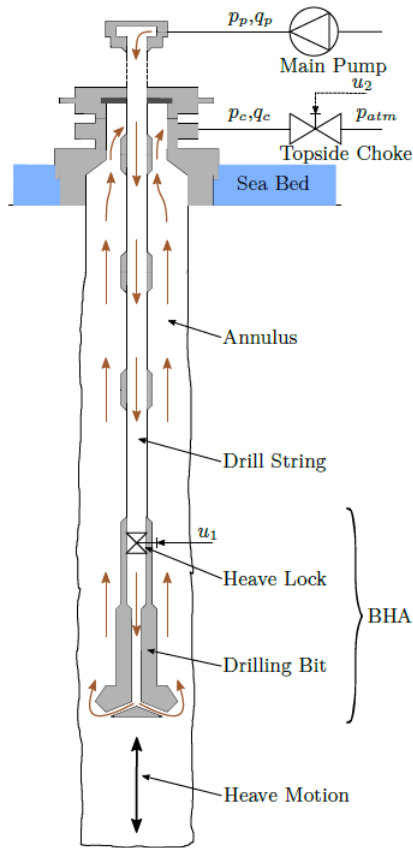


**Figure 2.1:** Setup of an offshore drilling system. The HeaveLock actuator is located above the *bit*. The figure is extracted from Schaut (2015).

to be fastened to the rig, and the drillstring will act as a piston in the well, causing pressure fluctuations in the downhole section, surpassing the upper and lower thresholds of the pressure window.

The HeaveLock project centers around a valve installed above the bit inside the drillstring as in Figure 2.1. This valve may be able to compensate for heave motion in the downhole section of the well; the objective of this thesis is to investigate this actuator during connections by simulation. A successful performance should encourage further testing and could eventually increase the efficiency of connections by cutting in shut-down costs and increasing the safety (Albert, 2013).



# CHAPTER 3

---

## Real Plant Simulator

---

In the following chapter, the mathematics of the Real Plant simulator is presented, the hydraulic well model, and the model of the bottom hole section, both reported from Schaut (2015). This gives a basis for understanding the simulation results later in Chapter 5 and 6. Real Plant is implemented in the programme MATLAB.

Real Plant was created parallelly with the IPT-Heave Lab, to foresee the Heave-Locks function in the real world. The simulation study is a part of this objective, especially as the lab is without a significant annulus, as this is disregarded.

The flow is assumed to be laminar and pressure difference and motion in the horizontal direction is negligible. Thermodynamic effects are also ignored (Aarsnes, 2012).

### 3.1 The hydraulic well model

In an oil well, there are two *conduits* to be considered - the annulus and the drill string - containing oil and drilling mud. These conduits can be modelled as two hydraulic transmission lines. The pressure and velocity of the pipe are also modelled and coupled with the transmission lines.

In total, there are six coupled PDE's governing the change in pressure and flow of the hydraulic well system, as well as the speed of the pipe. The PDE's are divided into three different areas of the well; the annulus, the pipe dynamics, and the pipes insides. The bottom of the well is defined as  $x = 0$ , and rig level is at  $x = L$ .

Heave motion of the wellbore, as well as the elasticity of the conduit, both contribute to surge and swab pressures in the downhole section of the well.

The annulus, modelled as a hydraulic transmission line

$$\frac{\partial p_a}{\partial t} = -\frac{\bar{\beta}_a}{A_a} \frac{\partial q_a}{\partial x} - \left( \frac{\bar{\beta}_a}{A_a} \frac{\partial A_a}{\partial p_i} \right) \frac{\partial p_i}{\partial t} \quad (3.1)$$

$$\frac{\partial q_a}{\partial t} = -\frac{A_a}{\rho} \frac{\partial p_a}{\partial x} - \frac{A_a}{\rho} F_a(q_a, v_p) + A_a g \cos(\theta_a(x)) \quad (3.2)$$

with the boundary conditions

$$q_a(t, 0) = q_r(t) + (A_{BHA} - A_i - A_p)v_{BHA} \quad (3.3)$$

$$q_a(t, L) = K_c \sqrt{p_a(t, L) - p_{atm}} \quad (3.4)$$

$\frac{\bar{\beta}_a}{A_a} \frac{\partial A_a}{\partial p_i}$  is the area change coefficient, describing the coupling between annulus cross section and pipe pressure inside the pipe, and is assumed to be constant.  $F_a(q_a, v_p)$  is a non-linear friction term depending on pipe velocity and annulus flow (Schaut, 2015).

The boundary condition 3.4 describes the flow at the top of the annulus and is determined by  $K_c$ , a constant opening of the topside choke and pressure differences at both sides of the choke.

Boundary condition 3.3 governs the flow at the bottom of the well and is determined by flow and volume change through the BHA.

As the fluid in the conduits can contract and expand, the bulk modulus is considered, given by Aarsnes et al. (2014), as presented in Mitchell (1988)

$$\bar{\beta}_a = \left( \frac{1}{A_a} \frac{\partial A_a}{\partial p_a} + \frac{1}{\beta} \right)^{-1} \quad (3.5)$$

Similarly to the annulus, the equations describing the dynamics inside of the pipe

$$\frac{\partial p_i}{\partial t} = -\frac{\bar{\beta}_i}{A_i} \frac{\partial q_i}{\partial x} - \left( \frac{\bar{\beta}_i}{A_i} \frac{\partial A_i}{\partial p_a} \right) \frac{\partial p_a}{\partial t} \quad (3.6)$$

$$\frac{\partial q_i}{\partial t} = -\frac{A_i}{\rho} \frac{\partial p_i}{\partial x} - \frac{A_i}{\rho} F_i(q_i, v_p) + A_i g \cos(\theta_i(x)) \quad (3.7)$$

with the boundary conditions

---

$$q_i(t, 0) = -q_p(t) \quad (3.8)$$

$$q_i(t, L) = -q_{bit}(t) + (A_i - A_{bit})v_{BHA} \quad (3.9)$$

The bulk modulus, used in equation 3.6, is defined as the bulk modulus of the annulus, in equation 3.5.

Here, the boundary condition at  $x = L$ , in equation 3.9, describing flow at rig level, is given by the negative of the flow supplied by the pump. The second boundary condition in equation 3.8, describing flow at the end of the pipe (position  $x = 0$ ), is defined by the flow through the bit and the volume changes caused by movement in the BHA.

The following PDE's describe the dynamics of the elastic pipe

$$\frac{\partial p_p}{\partial t} = -E \frac{\partial v_p}{\partial x} + f_i E \frac{\partial p_i}{\partial t} - f_a E \frac{\partial p_a}{\partial t} \quad (3.10)$$

$$\frac{\partial v_p}{\partial t} = -\frac{1}{\rho_p} \frac{\partial p_p}{\partial x} - \frac{1}{\rho_p} F_\rho(v_p, q_a, q_i) + g \cos(\theta_p(x)) \quad (3.11)$$

with the boundary conditions

$$v_p(t, 0) = v_{BHA}(t) \quad (3.12)$$

$$v_p(t, L) = v_{rig}(t) \quad (3.13)$$

The modeling of the pipe is reported from Aarsnes et al. (2014) where it is shown that the elastic pipe can exhibit resonant behaviour which significantly affects the downhole pressure.  $E$  is the pipe's Young modulus, which is the relationship between stress ( $\frac{F}{A}$ ) and proportional deformation in a material.  $f_i$  and  $f_a$  are the hoop-stress coefficients (Mitchell, 1988), describing a normal stress in the azimuth direction (PU, 2015).  $F_\rho$  is a friction term, which takes into account how the pipe walls exerts a viscous drag on the fluids inside and outside the pipe walls.

The boundary conditions, 3.12 and 3.13 set the speed of the pipe at end of pipe,  $x = 0$ , and at rig level,  $x = L$ .

### 3.1.1 Discretization

By letting the control volumes be of some finite non-zero length, the PDE is converted into a set of ODE's, giving an LTI system, allowing for standard control methods to be applied.

In Aarsnes et al. (2012) it was shown that accuracy is improved by increasing the number of control volumes, for a similar model to the one of this thesis. In the paper, the example of a 10000 m well is given, and acceptable performance was not achieved for  $N \leq 50$ . In the case described in this thesis, a well depth of 4000 m, a corresponding  $N \leq 20$  will not be sufficient. It is, therefore, desirable to have a relatively high number of control volumes. In later result chapters, the simulations are run using  $N = 30$  nodes.

### 3.1.2 Modeling the downhole section

The following section describes the modeling of the downhole pressure and movement, and is reported from Chapter 4 of Schaut (2015), where the deduction was made for the Heave Lab, and later transferred to the modeling of the real plant in Chapter 6.

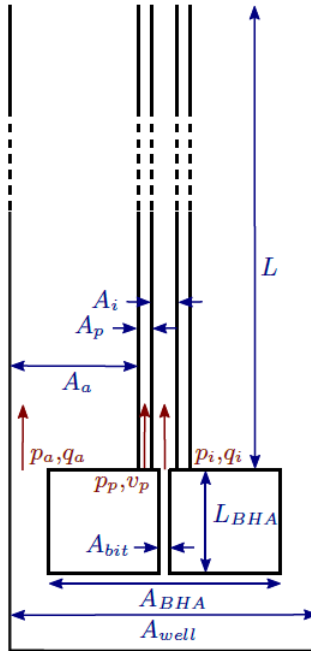


**Figure 3.1:** Model of the downhole section. The figure is extracted from Schaut (2015).

The downhole control volume is variable, depending on the BHA movement. If the downhole control volume is assumed to be the lower half of the down hole section, as shown in Figure 4.3 of Schaut (2015), it is given by the following equation

$$V_{dh} = \frac{V_{hole}}{2} + x_{BHA}A_{BHA} \quad (3.14)$$

$$\dot{V}_{dh} = v_{BHA}A_{BHA} \quad (3.15)$$

where  $x_{BHA}$  is the position, and  $v_{BHA}$  the velocity of the BHA.  $V_{hole}$  is the downhole control volume, where  $x_{BHA}$  is defined as zero in the middle of  $V_{hole}$ .  $A_{BHA}$  is defined as

$$A_{BHA} = \frac{\pi}{4}d_{BHA}^2 \quad (3.16)$$

The change in volume of the downhole section is given by the sum of influx and out flux, and also the change of the control volume. The mass balance of the downhole section;

$$\frac{d}{dt}mdh = \frac{d}{dt} \int \rho dV = \rho(q_{bit} - q_r) \quad (3.17)$$

where  $dh$  is the area change of the downhole section, given by the position of the bit,  $x_{bit}$ . The change in density over the volume,  $\int \rho dV$  is equal to  $V_{dh}\rho_{dh}$ , which can be expanded by the product rule for derivatives

$$\frac{d}{dt}(V_{dh} \times \rho_{dh}) = \dot{V}_{dh}\rho_{dh} + V_{dh}\dot{\rho}_{dh} \quad (3.18)$$

with  $\dot{\rho}_{dh} = \frac{\rho}{\beta}\dot{p}_{dh}$ , giving

$$\frac{d}{dt}(V_{dh} \times \rho_{dh}) = \dot{V}_{dh}\rho_{dh} + \frac{\rho}{\beta}V_{dh}\dot{p}_{dh} \quad (3.19)$$

Solving for downhole pressure,  $p_{dh}$  gives

$$\dot{p}_{dh} = \frac{\beta}{V_{dh}}(q_r - q_{bit} + \dot{V}_{dh}) \quad (3.20)$$

where  $V_{dh} = V_{hole} + x_{bit}A_{BHA}$ , and the change in downhole volume,  $\dot{V}_{dh} = (A_{BHA} - A_{bit})v_{BHA}$ , giving

$$\dot{p}_{dh} = \frac{\beta}{V_{hole} + x_{BHA}A_{BHA}}(q_r - q_{bit} + (A_{BHA} - A_{bit})v_{BHA}) \quad (3.21)$$

Movement of the BHA can be modelled by a balancing of forces in the BHA

---

$$\dot{v}_{BHA} = \frac{(A_{BHA} - A_{bit})p_{dh} - A_p p_p - (A_i - A_{bit})p_i(L) - (A_{BHA} - A_i - A_p)p_a(0)}{m_{BHA} - g - F_v(q_r, q_{bit}, v_{BHA})} \quad (3.22)$$

The friction term  $F_v(q_r, q_{bit}, v_{BHA})$  is due to the pressure drop through the BHA. Flow around the BHA is given by the non-linear equation

$$q_r = h_r(p_{dh} - p_a(t, 0)) \quad (3.23)$$

which is a function of the pressure difference between the downhole section and the section above. Similarly, flow through the drilling bit is given by the general non-linear equation

$$q_{bit} = h_{bit}(p_i(L) - p_{dh}) \quad (3.24)$$

depending on the pressure difference between the pipe's end and the downhole section.

## 3.2 The HeaveLock model

Figure 3.2 shows the mechanical design of the HeaveLock, from open on the left ( $u = 1$ ) to closed on the right ( $u = 0$ ). The figure gives an idea of why there would be a pressure drop through the HeaveLock, even at completely open, and why a lower and upper saturation are needed in the simulator.

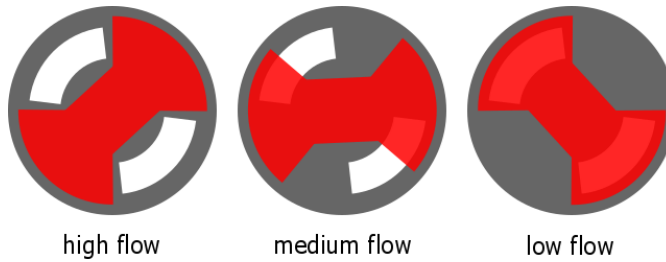


**Figure 3.2:** The mechanical design of the HeaveLock valve. The figure is extracted from Schaut (2015).

The existence of the HeaveLock in the simulator is implemented by a boundary condition which imposes a pressure drop between  $p_i(1)$  and  $p_i(0)$ . This is done to indicate the physical effects of a valve, as the HeaveLock can not be as non-restricting as a regular pipe, even at 100% opening. For a given HeaveLock opening,

$u$ , the corresponding free pipe area is  $A_{hl}(u)$ . For the cases explored in this thesis, the pressure drop is set to 50 bar at open. This may be unrealistic, but the actual level may only be determined after tests are done on the HeaveLock.

As the HeaveLock is located between the two nodes  $p_i(1)$  and  $p_i(0)$ , the flow through HeaveLock will be similar, but not equal to  $q_{bit}$ . Also depending on the opening, the flow through HeaveLock is

$$q_{hl} = k_{hl}(u_{hl})\sqrt{p_{hl,in} - p_{hl,out}} \quad (3.25)$$

where  $k_{hl}$  is the choke characteristic of the HeaveLock, which is calculated using the flow of continuous circulation,  $q_{cont} = 0.6q_{pump}$ , desired nominal HeaveLock opening

$$k_{hl} = \frac{q_{hl}}{u_{hl}\sqrt{p_{hl,in} - p_{hl,out}}} \quad (3.26)$$

In reality, the HeaveLock choke characteristic is complicated, however, in the Re-alPlant simulator,  $k_{hl}$  is simplified, modelled linearly;

$$k_{hl} = \frac{q_{cont}}{u_0\sqrt{p_{\Delta hl}}} \quad (3.27)$$

where  $u_0$  is the nominal HeaveLock opening, which the HeaveLock regulates around.

### 3.2.1 HeaveLock control

The desired HeaveLock opening is found by first calculating desired flow through the HeaveLock, and using that to calculate the needed opening.

In this continuous circulation case, the desired flow,  $q_{des}$  should be equal to the pump flow,  $q_{pump}$ , but for the HeaveLock to compensate for the surge and swab movement, the displacement of the BHA is used to find a new desired flow.

$$q_{des} = q_{pump} - v_{BHA}A_{bit} \quad (3.28)$$

where  $A_{bit}$  is the cross-sectional area of the bit. The desired flow is then used to calculate a new HeaveLock opening

$$u_{hl} = \frac{q_{des}}{k_{hl}\sqrt{p_{hl,in} - p_{hl,out}}} \quad (3.29)$$

The HeaveLock is also controlled by a saturation which only allows the HeaveLock opening to stay within a certain range,

$$u_{min} \leq u_{hl} \leq u_{max}$$

where  $u_{min}$  and  $u_{max}$  are defined as 0.05 and 1, for the cases that will be simulated in chapters 5 and 6, indicating respectively 5% and 100% opening.

# CHAPTER 4

---

## HeaveLock connection

---

The following chapter will consider challenges in activating and deactivating the HeaveLock's function, which will take place when connections are made and conventional heave compensation is not an alternative.

### 4.1 Simulation environment

Many simulations are to be done in this thesis in order to investigate the models theoretical real world behaviour. Most of the cases simulated in Chapters 5 and 6 use a case with well depth 4000 m and a continuous flow rate of  $2500 \frac{1}{m}$ . At the connection, the flow rate is ramped down to 60% -  $1500 \frac{1}{m}$ , for the time period when HeaveLock is active. Exceptions are made in Chapter 5 to look at the effect of varying well depth and flow rate.

For all cases, the given rig speed,  $v_{rig}$ , are real data from an anonymous rig. The rig speed is what causes the downhole piston movement, giving disturbances in the pressure. To be able to test for severe pressure changes,  $v_{rig}$  is scaled to give approximately  $\pm 10$  bar downhole.

The dimensions of the well can all be found in the simulator in the appendix, but some important sizes should be mentioned. The mass of the BHA is  $m = 400$  kg and the mud density is  $\rho = 1420 \frac{kg}{m^3}$ . The diameter of the exterior of the drillstring is 5.41 inches and the size of the hole is 7.36 inches. Readers experienced in

oil wells and their dimensions will from this information be able to contextualise results.

## 4.2 Conditions for making a connection

Using the HeaveLock system calls for a connection procedure. Certain pressure and flow conditions have to be changed from normal operation to an environment suitable for the HeaveLock.

The flow rate needs to be reduced, and this is done by linearly ramping it down, and later, up, after the connection is performed. The lowering of flow is necessary, but as a result, there is a pressure drop through the well. The pressure drop has to be balanced by partially closing the topside choke, where drilling fluid and oil exits the well. The closing and opening of the choke is also done by a linear ramp.

The decrease in flow rate is done, and the resulting pressure drop will reach the choke with a small delay. The same will happen as the choke closes, giving a surge in pressure. In summary, the following actions have to be taken before the HeaveLock is in a state where it can attenuate, listed in a somewhat arbitrary order

- flow rate is decreased (linearly ramped)
- the topside choke is partially closed (also linearly ramped)
- the HeaveLock opening is ramped down to the desired nominal value (again linearly)
- regular compensation techniques are turned off; heave attenuation is turned on (HeaveLocks regulator)

When these steps are completed and the right pressure and flow preconditions are set, the HeaveLock can start to operate. When it is ready, the conventional heave compensation are turned off.

After the connection is completed, a corresponding list of tasks have to be completed:

- flow rate is increased to the original value before the connection (linearly ramped)
- the topside choke is linearly ramped to fully open
- the HeaveLock opening is also linearly ramped up to fully open
- the HeaveLock is turned off and the regular heave attenuation compensation is turned on

**Table 4.1:** Time parameters which have to be defined for simulations.

| Variable            | Description   |
|---------------------|---|
| $t_{hl}^1$          | Time when HeaveLock starts to ramp down its opening from 1  |
| $\Delta t_{hl}^1$   | Duration of ramp down time for HeaveLock                    |
| $t_{hl}^{start}$    | Time when HeaveLock enters its active mode                  |
| $t_{hl}^{end}$      | Time when HeaveLock exits its active mode                   |
| $t_{hl}^2$          | Time when HeaveLock starts to ramp its opening back to 1    |
| $\Delta t_{hl}^2$   | Duration of ramp up time for HeaveLock                      |
| $t_p^1$             | Time when supply pump starts to ramp down the flow rate     |
| $\Delta t_p^1$      | Duration of ramp down time for pump                         |
| $t_p^2$             | Time when supply pump starts to ramp up the flow rate       |
| $\Delta t_p^2$      | Duration of ramp up time for pump                           |
| $t_c^1$             | Time when choke starts to close its opening                 |
| $\Delta t_c^1$      | Duration of ramp down time for choke                        |
| $t_c^2$             | Time when choke starts to open its opening                  |
| $\Delta t_c^2$      | Duration of ramp up time for choke                          |
| $t_{comp}^1$        | Time when conventional heave attenuation starts to turn off |
| $\Delta t_{comp}^1$ | Duration of phasing out of conventional heave attenuation   |
| $t_{comp}^2$        | Time when conventional heave attenuation starts to turn on  |
| $\Delta t_{comp}^2$ | Duration of phasing in of conventional heave attenuation    |

In the Real Plant simulator, the regular heave compensation used outside of connections is modelled in a simplified way. The regular heave compensation is modelled here simply as no disturbances as they are not the focus of this thesis.

In summary, the times listed in Table 4.1 have to be defined.

### 4.3 Initialization example

In this section, an example without disturbance is given. The time parameters of Table 4.1 are defined as in Table 4.2. All ramping times, marked  $\Delta$ , are set to 100 s.

Figure 4.1 shows the HeaveLock opening, flow rate and choke opening of the simulated example case. For the HeaveLock opening, the time from  $t = 300$  s to  $t = 400$  s is the ramping time. Outside the time interval of a connection being done, the HeaveLock is completely open.

Between  $t = 400$  s and  $t = 500$  s, the HeaveLock is kept at the nominal HeaveLock opening which in this example is set to  $u_0 = 0.4$ , and during this time, there is a build up of back pressure, which would be used for the regulation of flow through the HeaveLock if there were disturbances. At  $t = 500$  s the HeaveLock enters its active state.

**Table 4.2:** Time parameters defined for example in Section 4.3.

| Variable            | Value [sec] |
|---------------------|-------------|
| $t_{hl}^1$          | 300         |
| $\Delta t_{hl}^1$   | 100         |
| $t_{hl}^{start}$    | 500         |
| $t_{hl}^{end}$      | 800         |
| $t_{hl}^2$          | 900         |
| $\Delta t_{hl}^2$   | 100         |
| $t_p^1$             | 100         |
| $\Delta t_p^1$      | 100         |
| $t_p^2$             | 1200        |
| $\Delta t_p^2$      | 100         |
| $t_c^1$             | 200         |
| $\Delta t_c^1$      | 100         |
| $t_c^2$             | 1100        |
| $\Delta t_c^2$      | 100         |
| $t_{comp}^1$        | n/a         |
| $\Delta t_{comp}^1$ | n/a         |
| $t_{comp}^2$        | n/a         |
| $\Delta t_{comp}^2$ | n/a         |

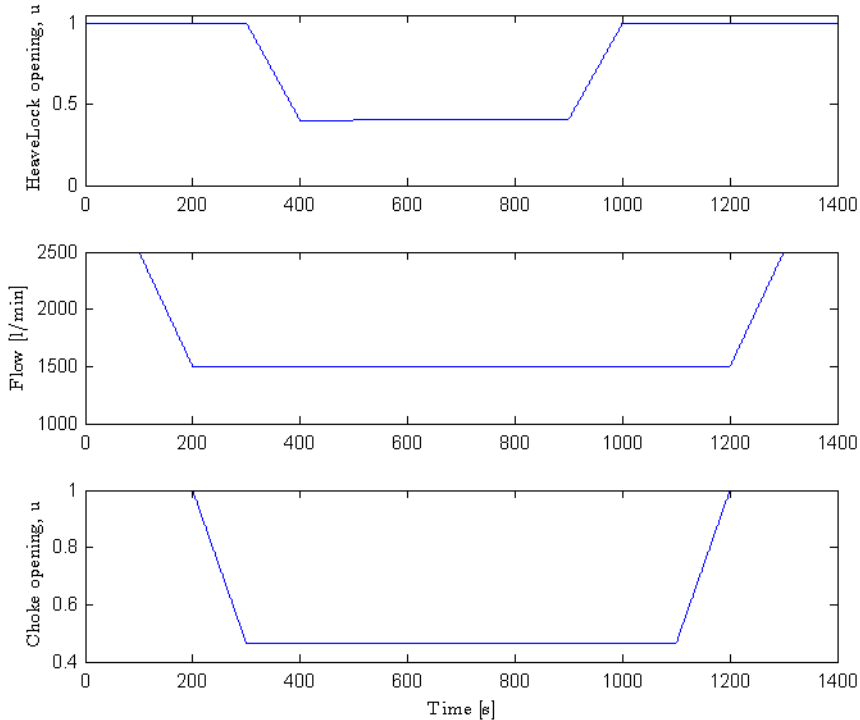
The ramping of the flow rate and choke opening are done before the HeaveLock enters its active state, and after it exits. The lowering of flow rate is a requirement of a typical connection, while the choke closing is a way to dampen pressure changes due to change in flow rate, and to maintain a continuous flow rate through the system.

Figure 4.2 shows the downhole pressure of the simulation. There are multiple surges and swabs in the pressure at levels around 10 bar, which is as high as the disturbances that are attempted attenuated in chapters 5 and 6. The largest pressure drops are one from  $t = 100$  s to  $t = 200$  s, where the downhole pressure reaches  $-7$  bar, and from  $t = 1100$  to  $t = 1200$  s where the downhole pressure reaches  $-8$  bar.

When the HeaveLock finishes its active state, at  $t = 800$  s, it merely holds the nominal HeaveLock opening until the time of ramping up is reached.

## 4.4 A successful connection

When doing connections for a real world well, the time that can be needed is normally in between 2 and 15 min; 120-960 s. The conditions described in the previous sections have to be in place for the HeaveLock to be in active mode, and



**Figure 4.1:** The HeaveLock opening, flow rate and choke opening, all as functions of time, for the exemplified simulation of Section 4.3.

the well should as quickly as possible be able to enter and exit the state for which these conditions are in place.

For a simulated case that could be feasible, achievable inputs and states have to be present. An important state is the pump pressure - whether the needed pump pressure is realistic. There are pressure restrictions for the pump, and, even more, strict restrictions for fixtures, and the pipe. A typical mud pump can supply up to about 500 bar (GardenDenver, 2016). As the maximum pressure allowed for fixtures is typically lower than for the pump, 500 bar can be used as a tentative limit of what simulation results that are realizable.

As the goal of the HeaveLock is to attenuate pressure surge and swab in the downhole section, it is important to check the downhole pressure,  $p_a(1)$ . For the cases presented in this thesis, heave motion causing pressure differences around  $\pm 10$  bar are tested for, and a tentative goal of the simulation study is to lower these oscillations to  $\pm 2 - 3$  bar. The disturbance is delivered by the rig speed,  $v_{rig}$ , converted to the speed of the BHA,  $v_{BHA}$ , mentioned in Section 3.1.2.

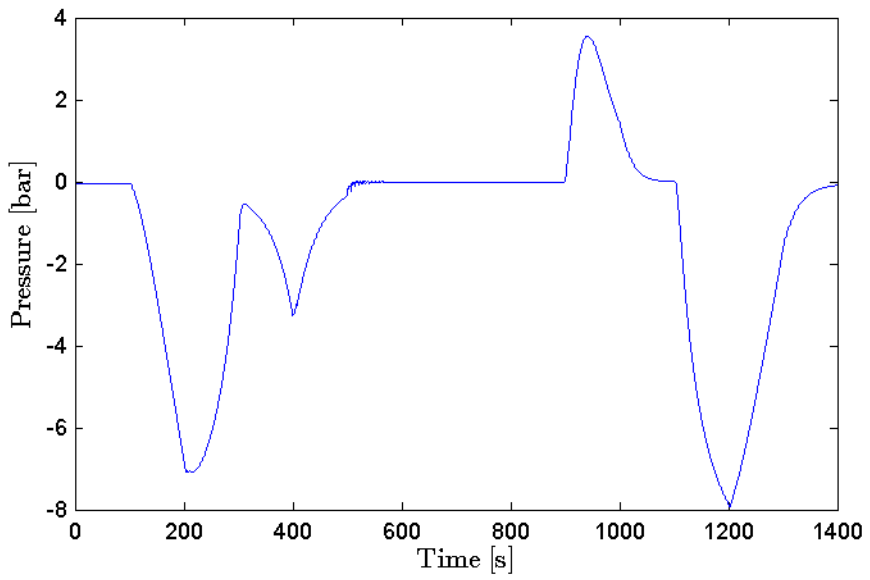


**Figure 4.2:** The downhole pressure as a function of time for the exemplified simulation of Section 4.3.

---

## Well Dimentions Effect on Simulations - Results

---

The Real Plant simulator was partly created to predict problems that could arise in utilising the HeaveLock, and the following chapter will explore some of the well dimensions effects on such simulations. This will give some insight into what physical conditions that theoretically will be acceptable for the usage of the HeaveLock in a real world subsea well.

The rig movement data used in this simulation study are from an anonymous installation. The samplings are taken over approximately 3 hours and as a normal connection will take 2 to 15 min, only fragments of the data is used. The data is scaled to give downhole pressure oscillations mainly in the area of  $\pm 10$  bar.

### 5.1 Nominal Heave Lock opening

The nominal HeaveLock opening,  $u_0$ , is an important tuning parameter for having a sufficient level of heave attenuation. The following cases are identical except for  $u_0$ . After the HeaveLock is initialized at  $t = 100$  s, regulation is made by the HeaveLock, which attempts to keep the HeaveLock opening around  $u_0$ .

#### Case 1a, $u_0 = 0.15$

Figure 5.1 shows the HeaveLock opening, downhole pressure difference and pump pressure for a simulation done over 800 s with pressure disturbance in the downhole

section of approximately  $\pm 10$  bar and nominal HeaveLock opening  $u_0 = 0.15$ . The HeaveLock does not enter saturation and the pump pressure is stable, but quite high, around 550 bar. As mentioned in Section 4.4, a pressure of more than 500 bar is probably not realizable. The corresponding downhole pressure difference is well regulated with a disturbance of predominantly  $\pm 2 - 3$  bar.

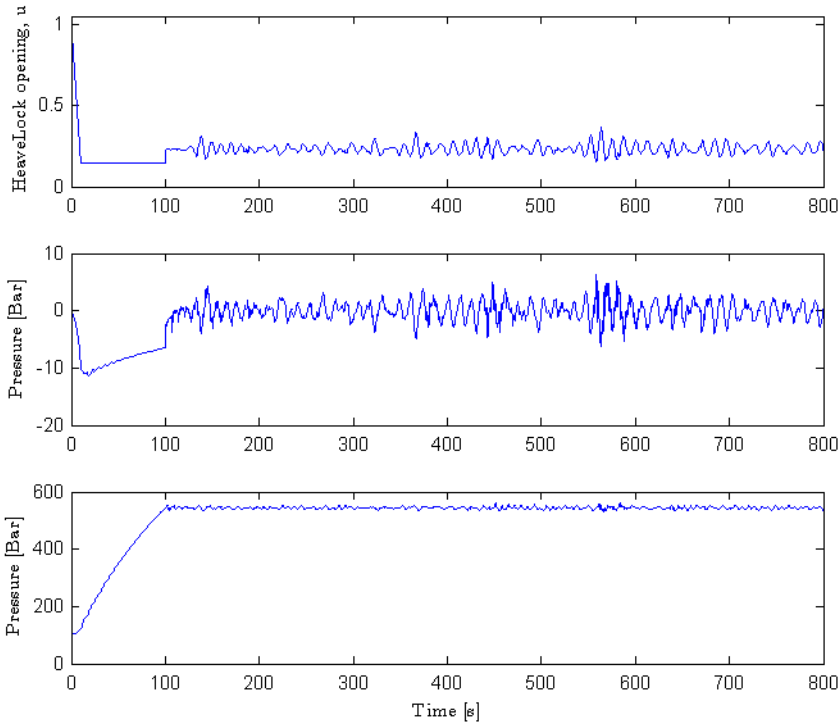


**Figure 5.1:** Case 1a, displaying the HeaveLock opening, downhole pressure difference and pump pressure, all as functions of time, of the simulation. The nominal HeaveLock opening is  $u_0 = 0.15$

### Case 1b, $u_0 = 0.3$

Figure 5.2 shows the HeaveLock opening, downhole pressure difference and pump pressure of Case 1b, simulated with the same conditions as Case 1a, but with a higher nominal HeaveLock opening of  $u_0 = 0.3$ . For the HeaveLock opening, it is apparent that it is not staying as tightly around the same value as for Case 1a, resulting in a lower pump pressure, of 300 bar. Both the pump pressure and the downhole pressure difference are also less strictly regulated. The HeaveLock opening barely enters the upper saturation limit once around  $t = 560$  s.

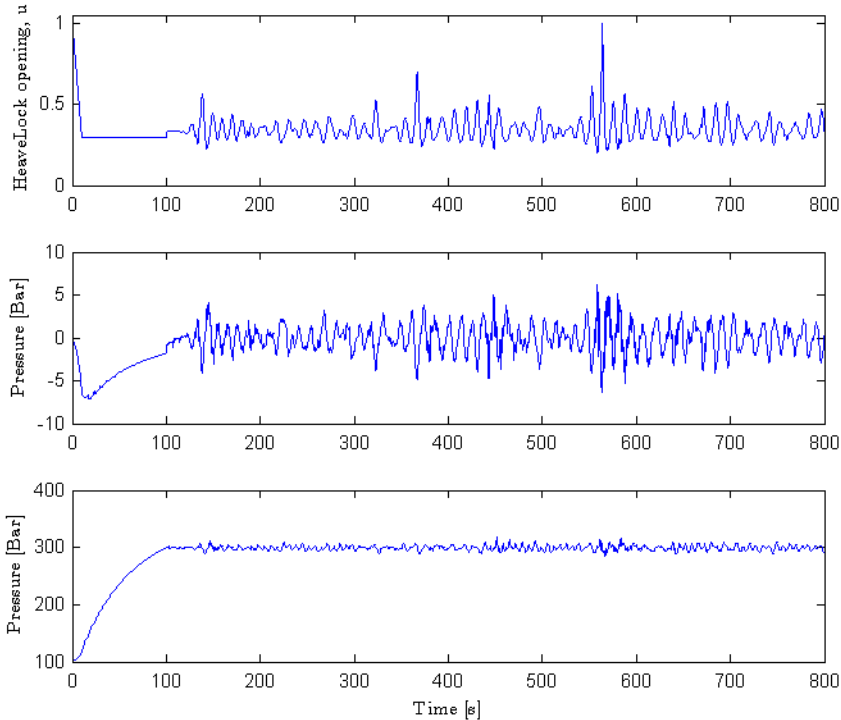


**Figure 5.2:** Case 1b, displaying the HeaveLock opening, downhole pressure difference and pump pressure, all as functions of time, of the simulation. The nominal HeaveLock opening is  $u_0 = 0.3$

### Case 1c, $u_0 = 0.5$

Case 1c is simulated with the same conditions as the two previous cases, Case 1a and 1b, but again with a new nominal HeaveLock opening,  $u_0 = 0.5$ . Figure 5.3 shows the HeaveLock opening, downhole pressure difference and pump pressure of the simulation, which shows that the system is not as well regulated as the two last cases, with disturbances around  $\pm 4$  bar in downhole pressure difference. Figure 5.3 also shows a lower pump pressure, which is now less stable, starting at around 180 bar, but drifting at times of severe HeaveLock saturation, and ending at 215 bar.

In these three cases, it is shown that a decreasing nominal HeaveLock opening gives a more accurate output; the HeaveLock can more easily regulate the downhole pressure, but this strongly affects the amplitude of the pump pressure. For an optimal result with virtually no pressure change downhole, it would require an extremely high pump pressure, which would be impossible in the real world.

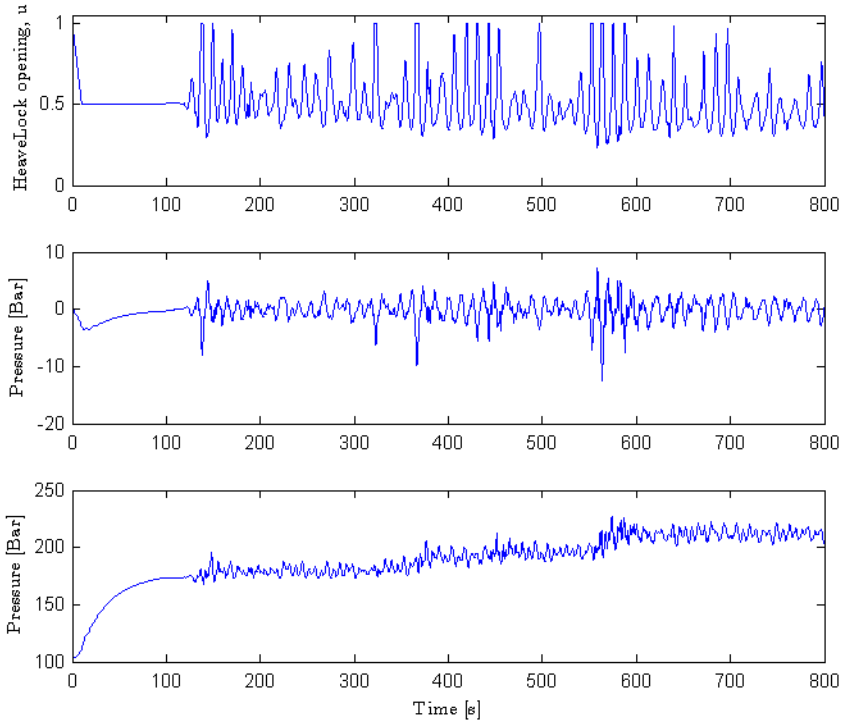


**Figure 5.3:** Case 1c, displaying the HeaveLock opening, downhole pressure difference and pump pressure, all as functions of time, of the simulation. The nominal HeaveLock opening is  $u_0 = 0.5$

## 5.2 Well depth

For an increasing well depth, the hypothesis is that the friction will eventually cancel the rig heave. For decreasing well depth, the friction will be less significant, and, therefore, require more pump pressure relative to depth.

Similarly to the cases from Section 5.1, the following simulation is done over 800 s, with HeaveLock active from  $t = 100$  s. The set nominal HeaveLock opening is  $u_0 = 0.4$ .

### Case 2a, $L = 1000$ m

The following case is simulated with a well depth of  $L = 1000$  m, which is a fourth of the given length for the rest of simulations in this thesis. Figure 5.4 shows the HeaveLock opening, downhole pressure and pump pressure of the simulation. The

downhole pressure is oscillating around about 147 bar. The pump pressure starts at  $\sim 200$  bar, drifts a little around  $t = 360$  s and  $t = 560$  s, and ends at  $\sim 240$  bar.

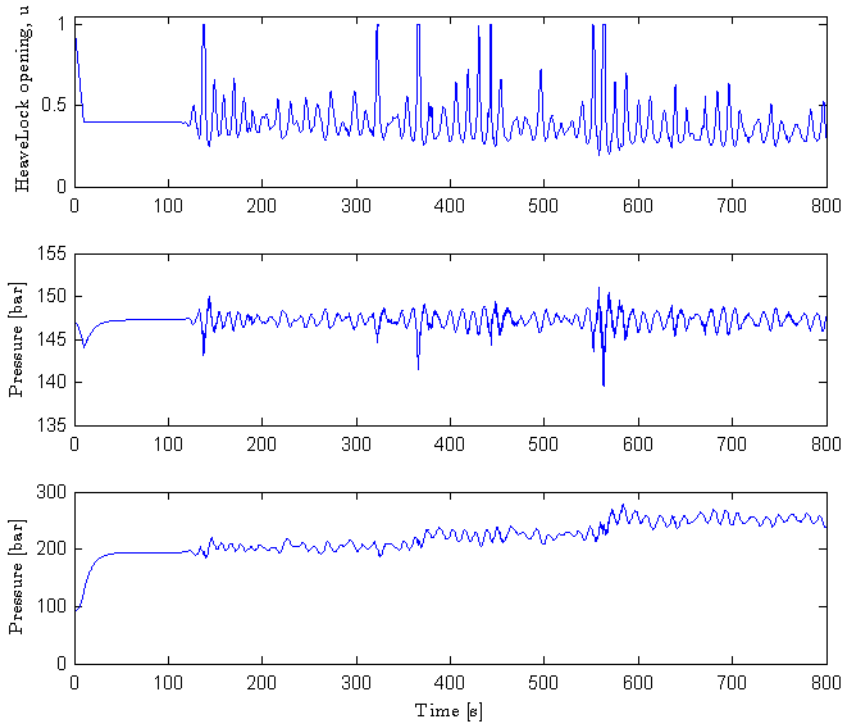


**Figure 5.4:** Case 2a, displaying the HeaveLock opening, downhole pressure and pump pressure, all as functions of time, of the simulation. The well depth is  $L = 1000$  m.

### Case 2b, $L = 4000$ m

Figure 5.5 depicts the simulation with well depth  $L = 4000$  m, which is the set well length that the HeaveLocks function is tested for in all but the two surrounding cases. Figure 5.5 shows a set of graphs for the simulation; the HeaveLock opening, downhole pressure difference and the pressure supplied by the pump. Naturally, the downhole pressure is higher for this case varying around  $\sim 556$  bar, as the column of drilling fluids in the pipe is of greater weight and volume the longer it gets. The pump pressure is drifting less.

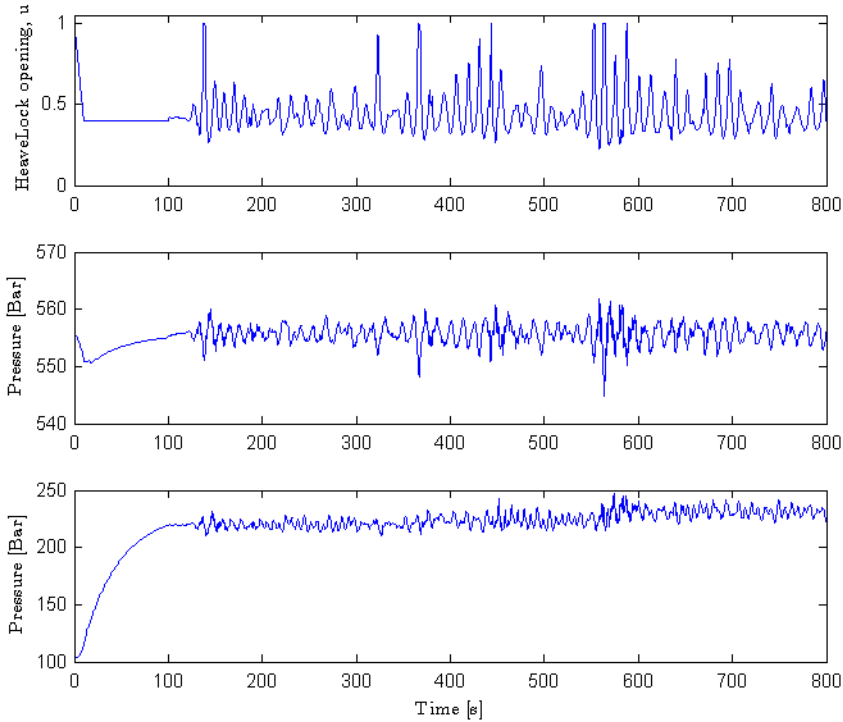


**Figure 5.5:** Case 2b, displaying the HeaveLock opening, downhole pressure and pump pressure, all as functions of time, of the simulation. The well depth is  $L = 4000$  m.

### Case 2c, $L = 10000$ m

To examine the effects of a deeper well, a case with well depth  $L = 10000$  m is simulated. In Figure 5.6, the HeaveLock opening, downhole pressure and pump pressure are shown. Although the regulation seems to be worse here, judging by the regulation of the downhole pressure and the HeaveLock entering saturation slightly more frequently than in Case 2a, the pump pressure does not drift, indicating that the regulation might still be better than for the short well length.

The pump pressure is again raised from Case 2b, and is at a level of 1370 bar, as a result of the higher weight column above the BHA.

Figures 5.7 shows the speed of the BHA of the three cases; 2a, 2b and 2c. The speed stays around the same level of about  $\pm 1.5 - 2 \frac{\text{m}}{\text{s}}$ , however, the short well, simulated in Case 1a is varying more than the two other cases which confirm the hypothesis that for a deeper well, friction will cancel out some movement.

It is quite difficult to decide which well depth gives a better regulation. For the long

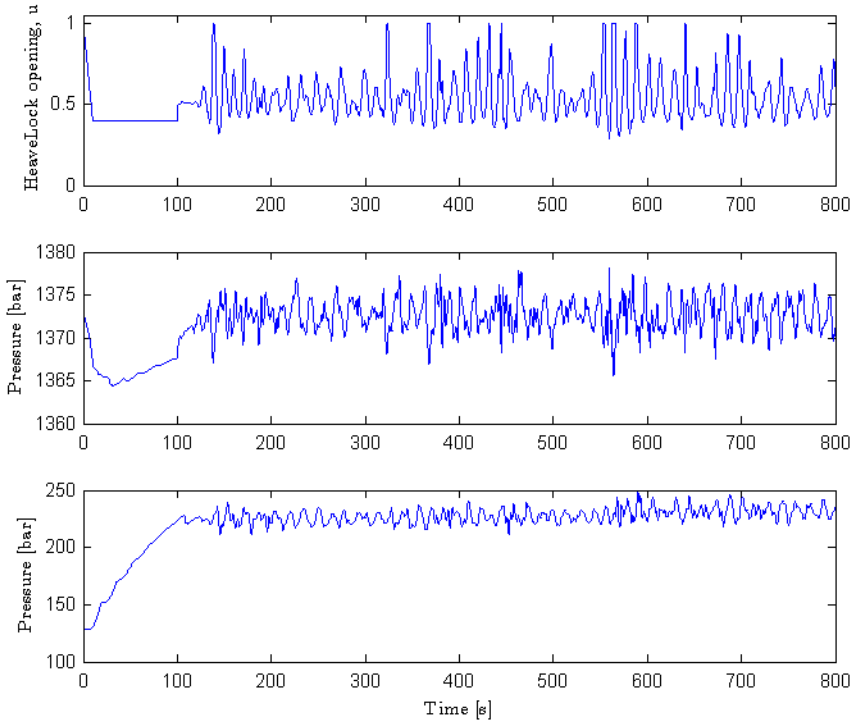


**Figure 5.6:** Case 2c, displaying the HeaveLock opening, downhole pressure and pump pressure, all as functions of time, of the simulation. The well depth is  $L = 10000$  m.

well, simulated in Case 2c, there will be a longer time delay, which the HeaveLock might have difficulty handling. As the pipe is substantially longer than for cases 2a and 2b, the friction through the well constrains the movement of the pipe and the wellhead, dampening the heave motion, which might make up for the time delay.

While it is interesting to look at the effects of well depth, it is not a parameter that can be changed, and so for the rest of simulations, well depth is set to  $L = 4000$  s.

## 5.3 Flow rate

For an active sequence of the HeaveLock, an increase or decrease in flow rate should in theory not be a problem. For a lower flow rate, however, a smaller nominal HeaveLock opening will be needed to keep sufficient back pressure.

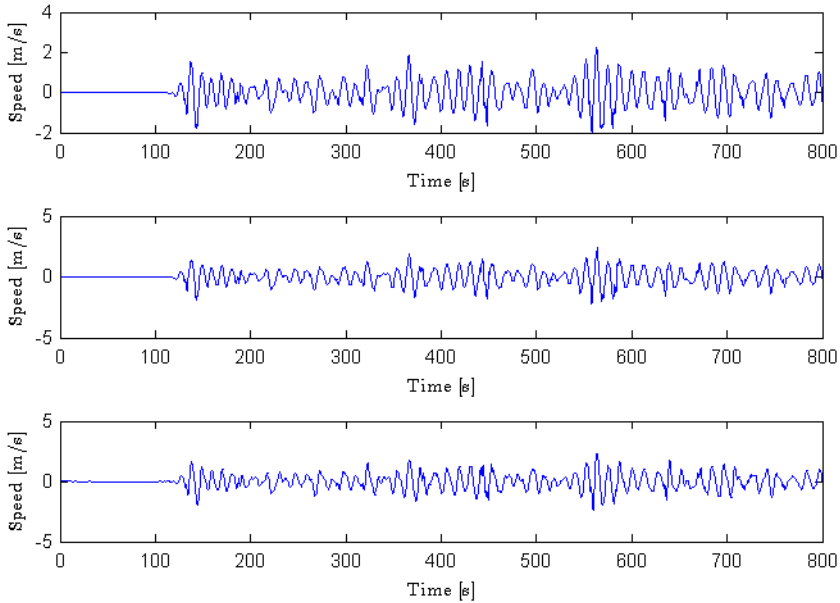


**Figure 5.7:** Case 2a, b and c, displaying the speed of the BHA,  $v_{BHA}$  for the three cases, as functions of time.

In this section, three different flow rates will be tested for. All parameters except the flow rate are unaltered (nominal HeaveLock opening  $u_0 = 0.4$ ). These simulations are made to investigate the effects of flow rate on the HeaveLock.

### Case 3a, $q = 600 \frac{1}{\text{min}}$

The first simulation is made using the continuous flow rate  $q = 600 \frac{1}{\text{min}}$ . Figure 5.8 displays the HeaveLock opening, downhole pressure and the pump pressure.

In the first sub-figure, the HeaveLock opening is shown. It saturates multiple times, and there is a resulting drift in the pump pressure. The pump pressure is quite low, around 50 – 90 bar. The regulation of the downhole pressure varies around  $\pm 4$  bar.

### Case 3b, $q = 2500 \frac{1}{\text{min}}$

The second case is made using the given flow rate  $q = 0.6 * q_{\text{pump}} = 1500 \frac{1}{\text{min}}$ . Later, in Chapter 6 the initial flow rate  $2500 \frac{1}{\text{min}}$  is ramped down to  $1500 \frac{1}{\text{min}}$  before

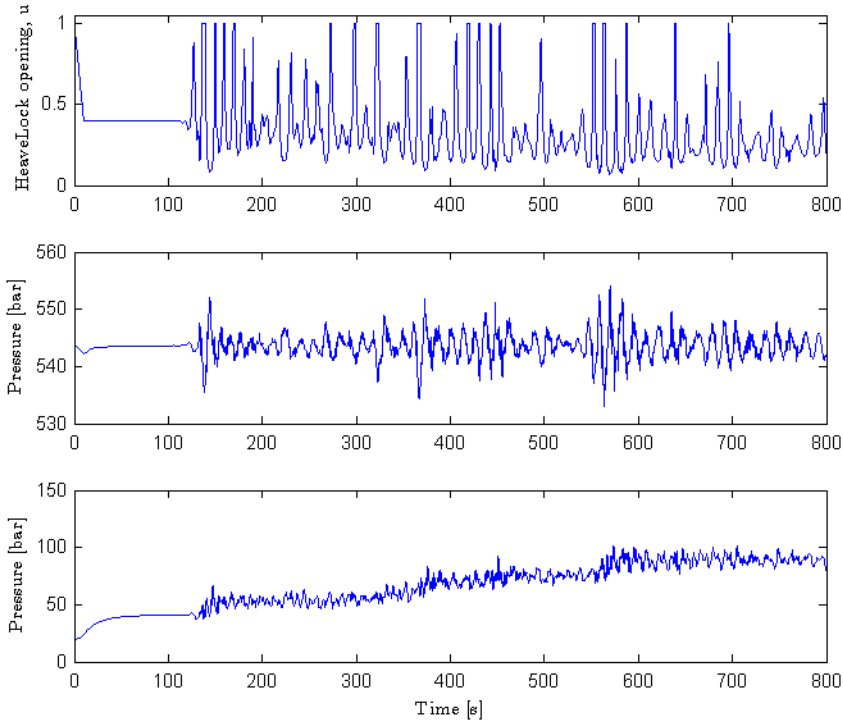


**Figure 5.8:** Case 3a, displaying the HeaveLock opening, downhole pressure and pump pressure, all as functions of time, of the simulation. The continuous flow rate is  $q = 600 \frac{1}{\text{min}}$ .

the HeaveLock is active, and this is the reason  $1500 \frac{1}{\text{min}}$  is used as an example for the current case. This case is in fact the same one as Case 2b. It is re-entered in order to contextualize the surrounding cases, 3a and 3c.

Figure 5.9 shows the HeaveLock opening, downhole pressure difference and pump pressure of the simulation. Compared to Case 3a, the downhole pressure is more well-regulated for the current case. The HeaveLock opening does not saturate as many times - only 6 times, compared to 17 times for Case 3a during the same wave sequence. As a result, the disturbance in downhole pressure mainly fluctuates around  $\pm 2.5$  bar.

The pump pressure of the simulation is higher for this case, starting at  $\sim 220$  bar, drifting especially at  $t \approx 570$  s ending at 233 bar.

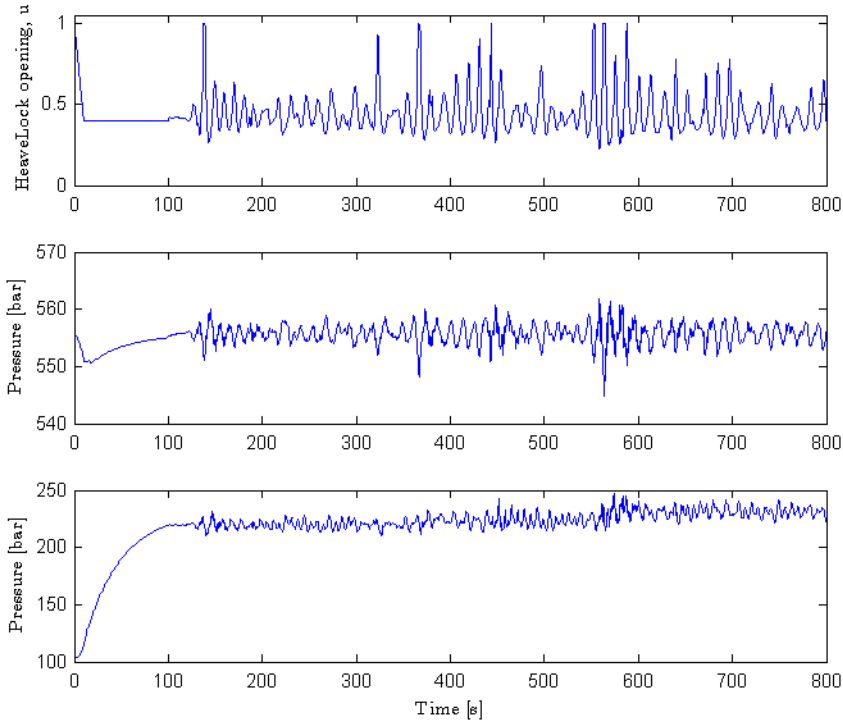


**Figure 5.9:** Case 3b, displaying the HeaveLock opening, downhole pressure and pump pressure, all as functions of time, of the simulation. The continuous flow rate is  $q = 1500 \frac{1}{\text{min}}$ .

### Case 3c, $q = 3000 \frac{1}{\text{min}}$

Case 3c is simulated using a higher flow rate of  $3000 \frac{1}{\text{min}}$ . The effect of this on the HeaveLock opening, downhole pressure and pump pressure are displayed in Figure 5.10.

In the figure, it is apparent that the HeaveLock opening never saturates, for the same sequence of disturbance in which cases 3a and b went into saturation 6 and 17 times, respectively. Despite this, there is not a large difference in downhole pressure, the regulation is only slightly more strict, although the mean level is about 35 bar higher for this case than for Case 3b.

The pump pressure, however, is approximately 750 bar, which is unrealistically high, both for the pump, for which the max allowed pressure is around 500 bar and for fixtures, which probably can tolerate even less.

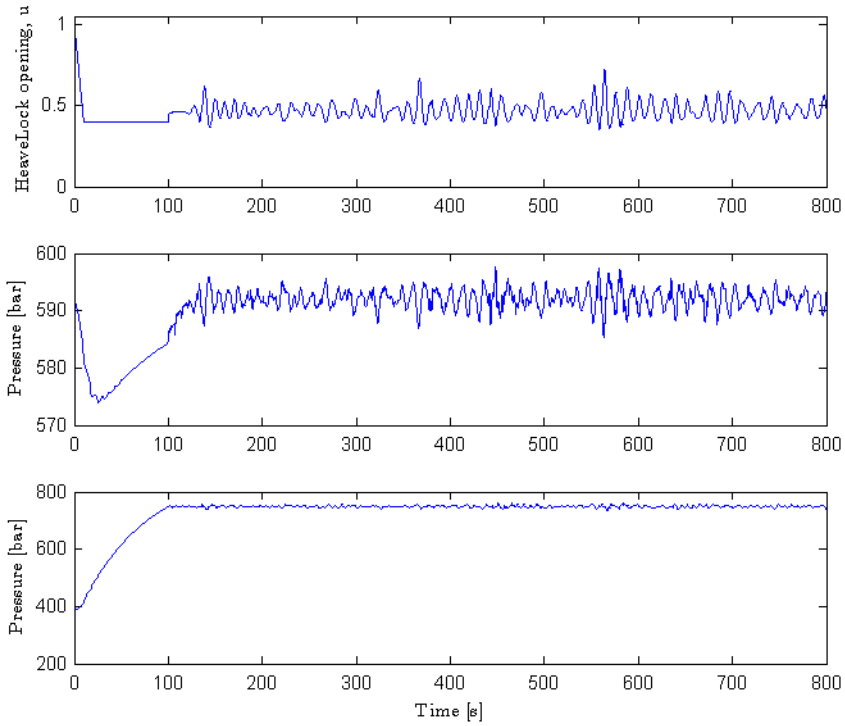


**Figure 5.10:** Case 3c, displaying the HeaveLock opening, downhole pressure and pump pressure, all as functions of time, of the simulation. The continuous flow rate is  $q = 3000 \frac{1}{\text{min}}$ .



---

## Connection simulations - Results

---

Many parameters can be changed in the RealPlant simulator. There are a lot of time parameters, especially which can have an effect on the downhole pressure. In this chapter, the altering of some parameters is demonstrated, to give an impression of their effect.

As mentioned in Section 3.2, the pressure drop at open is set to 50 bar, but this may in fact not be the case in reality. Further investigation is needed on the actual drop, and should be done by physical inspection of the HeaveLock valve.

### 6.1 Connection simulation example

Table 6.1 shows a table, similar to Table 4.2, but here with overlapping ramps for the HeaveLock, pump flow and topside choke opening. By having overlaps, some of the undesired effects of the ramps on the downhole pressure are cancelled out. As mentioned earlier, it also saves time. The ramps are overall shortened to 80 s for the ramping down and later ramping up, of both the flow rate and the choke opening.

Figure 6.1 shows the downhole pressure of the simulation compared to the downhole pressure without the HeaveLock. Although it can be somewhat difficult to make out the disturbances that are in the area of  $\pm 10$  bar for the no-HeaveLock case, are in the area of  $\pm 3.5$  bar for the HeaveLock case.

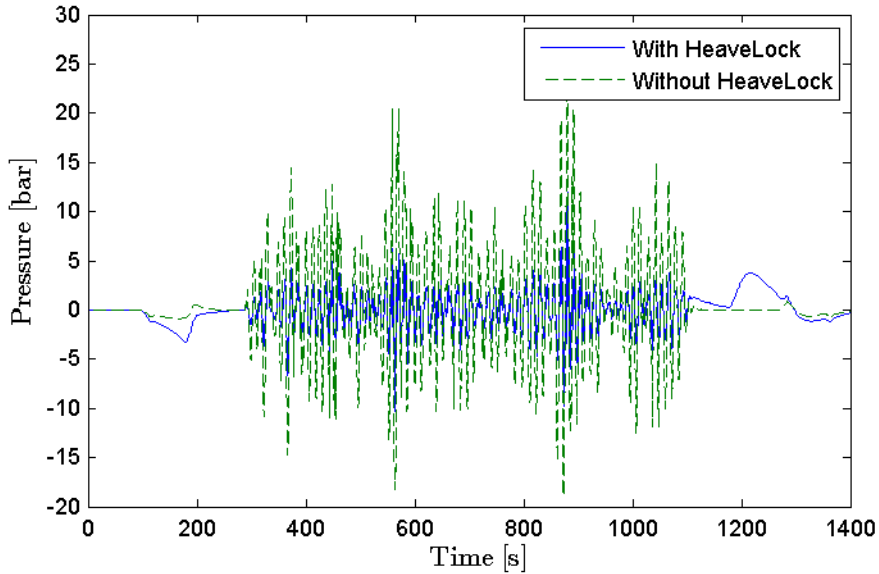


**Figure 6.1:** Connection example case, displaying the downhole pressure difference of the case compared to the same case without the use of HeaveLock, as functions of time.

The HeaveLock opening, flow rate and choke opening are shown in Figure 6.2 to give an impression of when ramping of inputs are performed. As mentioned, the ramps are now somewhat overlapping.

## 6.2 HeaveLock ramping time

In the following two cases, experimenting with  $\Delta t_{hl}^1$  and  $\Delta t_{hl}^2$ , the ramping times at initialization and termination of the HeaveLock is done to investigate its effect on the well parameters. The following three cases; 4a, b and c are connections lasting about 850 s.

It is quite hard to differentiate between the downhole pressure disturbance with and without the HeaveLock, as shown in Figure 6.1. Only the downhole pressure regulated by the HeaveLock will be shown in this chapter, although the rig moving sequence is the same as the one used for the example connection case in the above section.

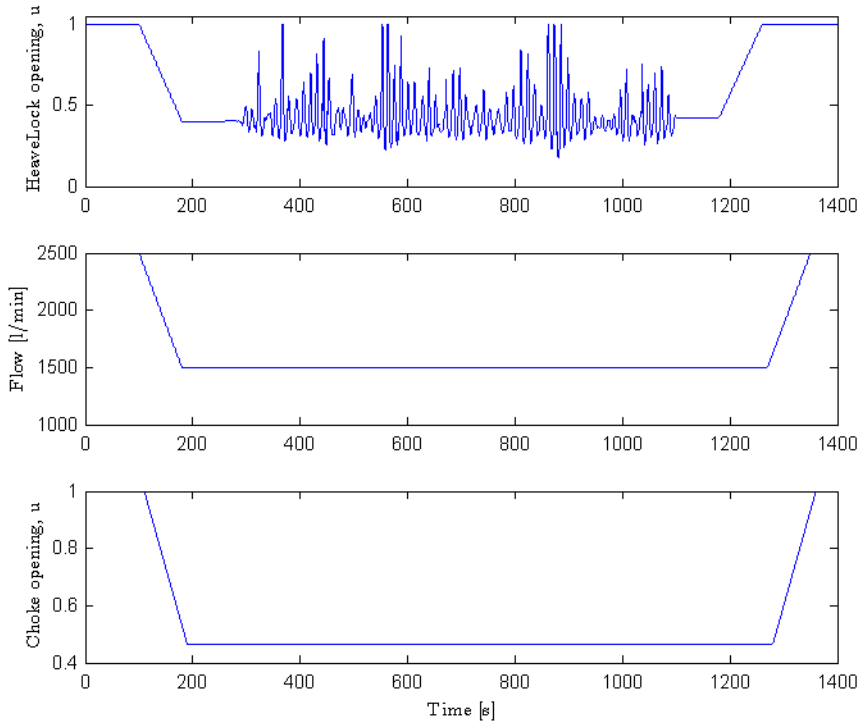


**Figure 6.2:** Connection example case, displaying the HeaveLock opening, flow rate and choke opening, all as functions of time, of the simulation.

**Table 6.1:** Time parameters defined for example in Section 6.1.

| Variable            | Value [sec] |
|---------------------|-------------|
| $t_{hl}^1$          | 100         |
| $\Delta t_{hl}^1$   | 80          |
| $t_{hl}^{start}$    | 260         |
| $t_{hl}^{end}$      | 1100        |
| $t_{hl}^2$          | 1180        |
| $\Delta t_{hl}^2$   | 80          |
| $t_p^1$             | 100         |
| $\Delta t_p^1$      | 80          |
| $t_p^2$             | 1270        |
| $\Delta t_p^2$      | 80          |
| $t_c^1$             | 110         |
| $\Delta t_c^1$      | 80          |
| $t_c^2$             | 1280        |
| $\Delta t_c^2$      | 80          |
| $t_{comp}^1$        | 280         |
| $\Delta t_{comp}^1$ | 30          |
| $t_{comp}^2$        | 1080        |
| $\Delta t_{comp}^2$ | 30          |

**Case 4a,  $\Delta t_{hl} = 20$  s**

Case 4a is simulated using a short ramping interval for the HeaveLock of  $\Delta t_{hl}^1 = \Delta t_{hl}^2 = 20$  s. The ramping down of the HeaveLock opening happens in the time interval from 100 s to 120 s, and the ramping up happens in the interval 1180 s to 1200 s.

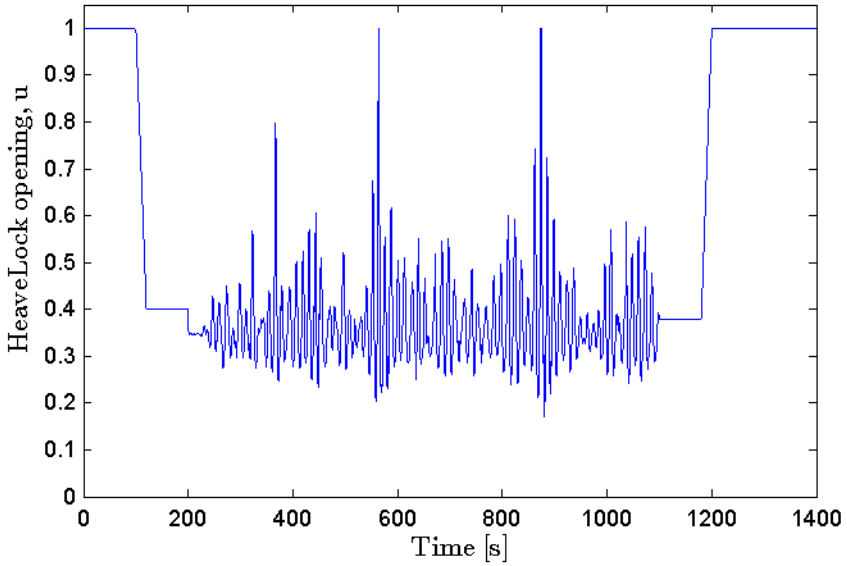
In Figure 6.3, displaying the HeaveLock opening for the simulation, the ramps are looking quite similar to vertical lines; the HeaveLock opening is ramped rapidly.

Figure 6.4, showing the downhole pressure difference for the simulation, demonstrates the effect of this, and pressure disturbances are reaching  $\approx -7$  bar and  $\approx 9.5$  bar due to the ramping of the HeaveLock opening.

**Case 4b,  $\Delta t_{hl} = 100$  s**

For this case, the HeaveLock ramping times are set to  $\Delta t_{hl}^1 = \Delta t_{hl}^2 = 100$  s. The resulting HeaveLock opening and downhole pressure difference are presented in Figures 6.5 and 6.6. The HeaveLock is initialized at  $t_{hl}^1 = 100$  s, finishing at  $t = 200$  s and terminated from  $t_{hl}^2 = 1180$  s to  $t = 1280$  s.

Compared to Figure 6.4, Figure 6.6 shows a far lower disturbance in downhole pressure due to the ramping of the HeaveLock opening, with pressure surges reaching



**Figure 6.3:** Case 4a, the HeaveLock opening of the connection simulation, as a function of time, with  $\Delta t_{hl}^1 = \Delta t_{hl}^2 = 20$  s.

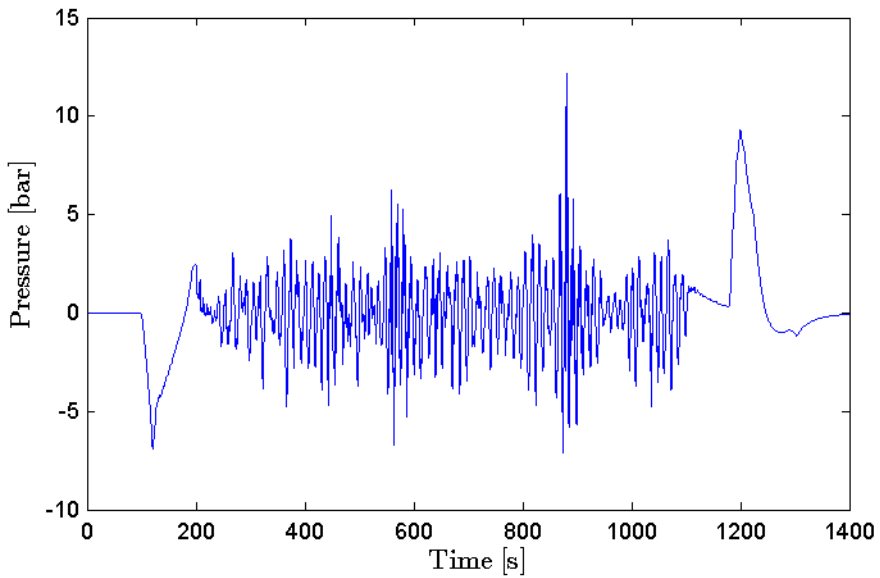


**Figure 6.4:** Case 4a, the downhole pressure difference of the connection simulation, as a function of time, with  $\Delta t_{hl}^1 = \Delta t_{hl}^2 = 20$  s.

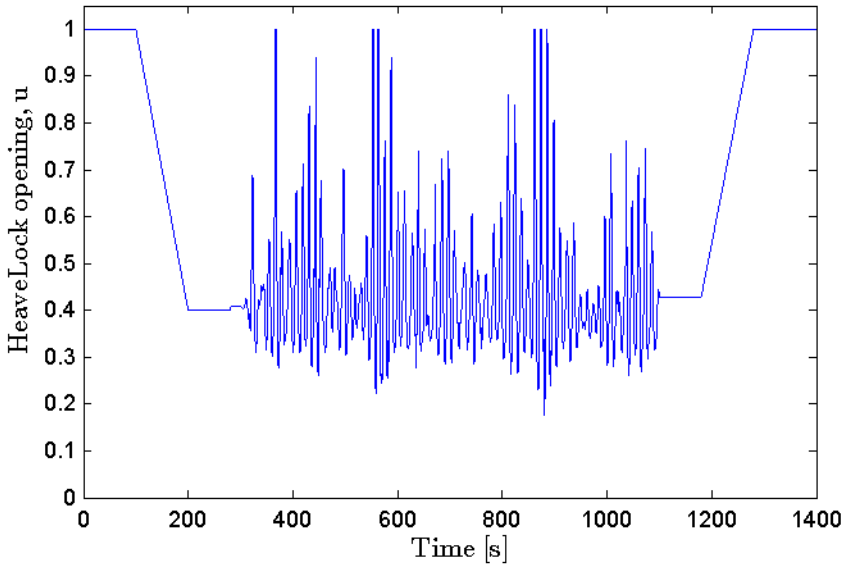


**Figure 6.5:** Case 4b, the HeaveLock opening of the connection simulation, as a function of time, with  $\Delta t_{hl}^1 = \Delta t_{hl}^2 = 100$  s.

$\approx -1.7$  bar and  $\approx 3.2$  bar.

### Case 4c, $\Delta t_{hl} = 150$ s

The third case, 4c, has the longest HeaveLock ramp time of  $\Delta t_{hl}^1 = \Delta t_{hl}^2 = 150$  s. The ramping down of the HeaveLock opening happens in the time interval from 100 s to 250 s, and the ramping up happens in the interval 1180 s to 1330 s.

Figure 6.7 shows the HeaveLock opening of the simulation, with a more slanted ramp than the two previous cases. In Figure 6.8 the corresponding downhole pressure changes are presented, showing ramping pressure surges in the downhole are dramatically lowered to  $\approx -2.5$  bar and  $\approx 2.5$  bar which can be considered within the acceptable range. Strangely, the initial pressure peak is smaller for Case 4b ( $\approx -1.7$  bar). This is probably due to the positioning of the HeaveLock ramp relative to the ramping of the choke and the flow.

For the third case, the HeaveLock also seems to have slightly more difficulty in the regulation, although not much. As the consequences of lowering the ramping times to, for example, 20 s, are too high, and the regulation is not largely affected, this is not considered in the choice of ramping times.

For a real world well, it is desired to have the shortest possible ramping in and out of the HeaveLock, while giving an acceptable downhole pressure. A ramping

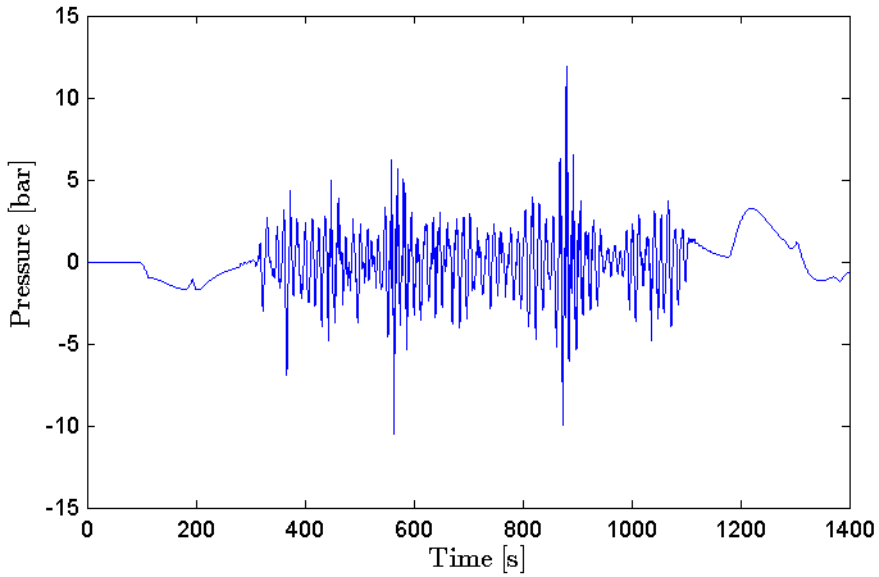


**Figure 6.6:** Case 4b, the downhole pressure difference of the connection simulation, as a function of time, with  $\Delta t_{hl}^1 = \Delta t_{hl}^2 = 100$  s.

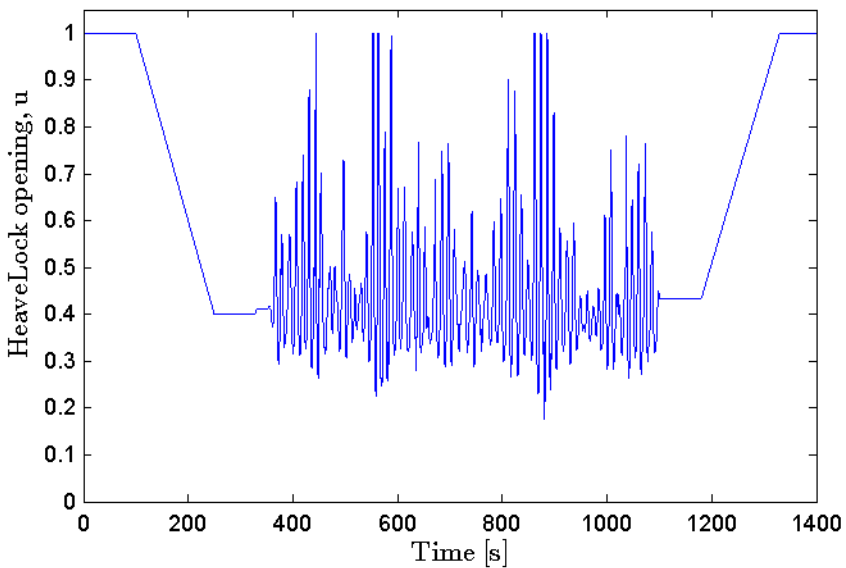


**Figure 6.7:** Case 4c, the HeaveLock opening of the connection simulation, as a function of time, with  $\Delta t_{hl}^1 = \Delta t_{hl}^2 = 150$  s.

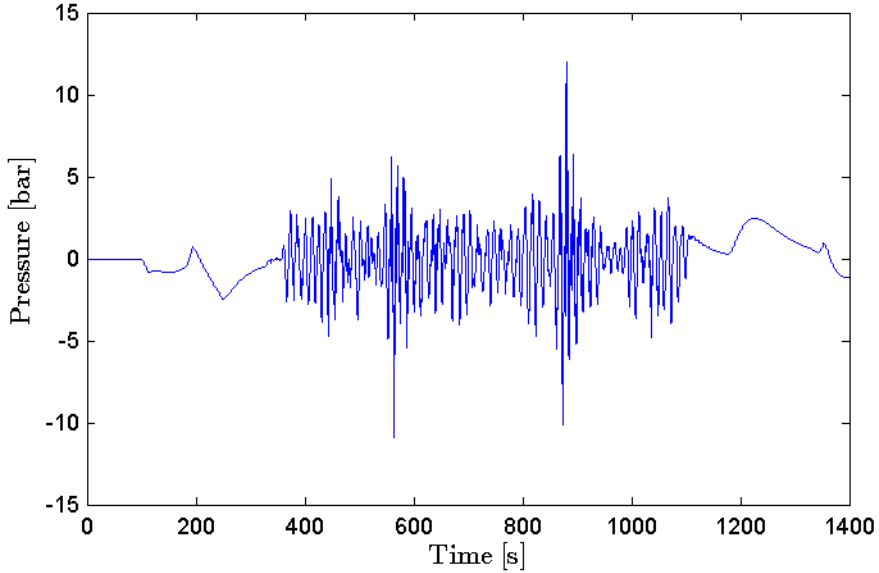


**Figure 6.8:** Case 4c, the downhole pressure difference of the connection simulation, as a function of time, with  $\Delta t_{hl}^1 = \Delta t_{hl}^2 = 150$  s.

time of  $\Delta t_{hl}^1 = \Delta t_{hl}^2 = 100$  s is used for the remaining simulations despite the peak in downhole pressure at ramping up of the HeaveLock opening, as increasing this ramping time does not largely affect the simulation, and naturally takes up more time.

### 6.3 HeaveLock build up time

In this section, the altered parameter is the wait time between the initial ramping of the HeaveLock and the activation of the HeaveLock; the time period  $t_{hl}^{buildup} = t_{hl}^{start} - t_{hl}^1 - \Delta t_{hl}^1$ . This time period is named  $t_{hl}^{buildup}$  as it is the time the nominal HeaveLock opening,  $u_0 = 0.4$ , is held, and the system has the time to build up back pressure, used in regulating the flow  $q_{des}$ , once the HeaveLock is activated.

The following three cases; 5a, b and c are connections lasting about 850 s.

**Case 5a,**  $t_{hl}^{buildup} = 20$  s

Case 5a is simulated using a build up time  $t_{hl}^{buildup} = 20$  s. Figure 6.9 shows the HeaveLock opening of the simulation. The build-up interval takes place from the end of the initial ramping of the HeaveLock, at  $t = 200$  s, to the activation of

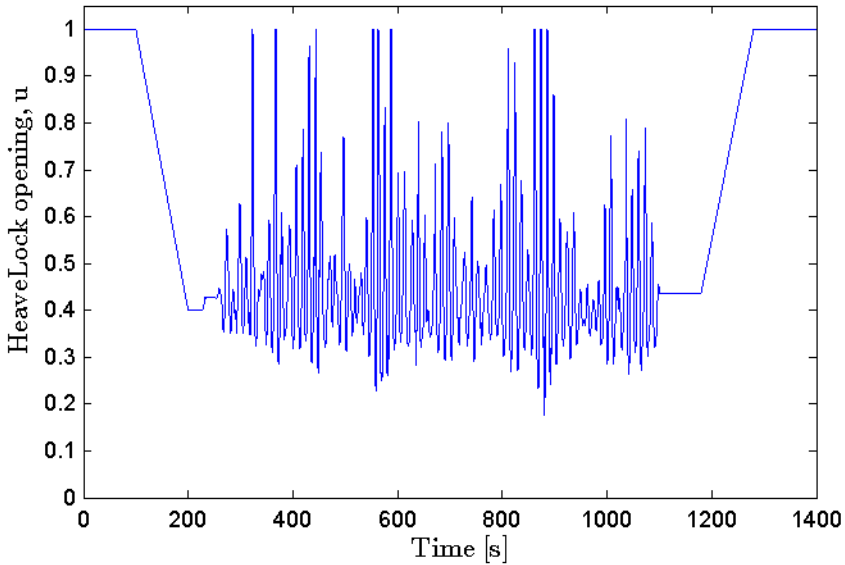


**Figure 6.9:** Case 5a, the HeaveLock opening of the connection simulation, as a function of time, with  $t_{hl}^{buildup} = 30$  s.

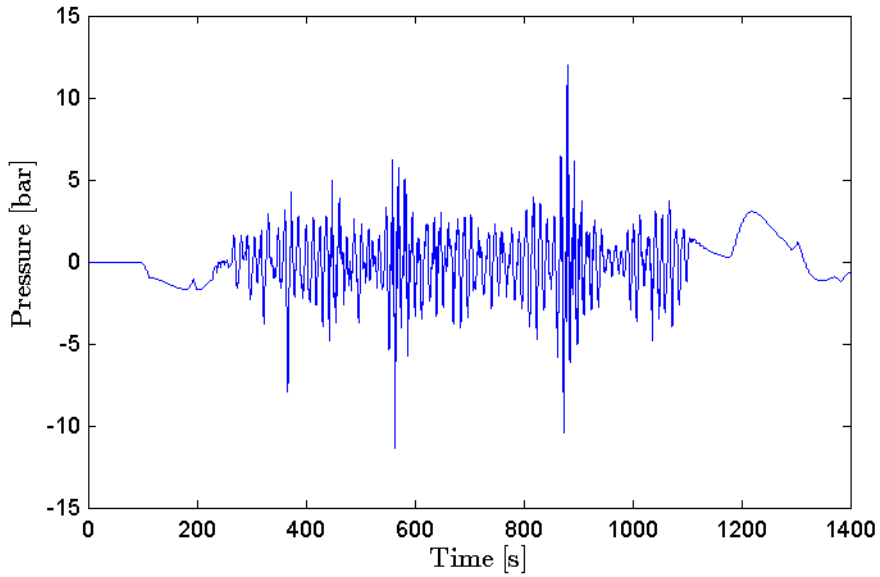
the HeaveLock, at  $t = 220$  s. The HeaveLock opening enters saturation a few times.

Figure 6.10 shows the corresponding downhole pressure of the simulation, which seems not to be oscillating a lot. As previously mentioned, pressure oscillations around  $\pm 10$  bar without the use of the HeaveLock should be able to keep within the  $\pm 2 - 3$  bar range, while, for the current case, pressures around  $\approx 3 - 4$  bar are apparent.

### Case 5b, $t_{hl}^{buildup} = 100$ s

The build-up interval,  $t_{hl}^{buildup}$  is increased to 100 s for the second case. The tracked HeaveLock opening is shown in Figure 6.11, with the interval between  $t = 200$  s to  $t = 300$  s. The resulting downhole pressure changes are shown in Figure 6.12.

The downhole pressure difference and HeaveLock opening of the simulation seem more well-regulated for this case, demonstrating lower pressure oscillations now mainly around  $\pm 2.5$  bar. The HeaveLock is for the current case increasingly able to handle the pressure changes, in Figure 6.11 the HeaveLock is saturated a fewer amount of times than in Case 5a and seems to stay more around the nominal HeaveLock opening,  $u_0 = 0.4$ .



**Figure 6.10:** Case 5a, the downhole pressure difference of the connection simulation, as a function of time, with  $t_{hl}^{buildup} = 30$  s.

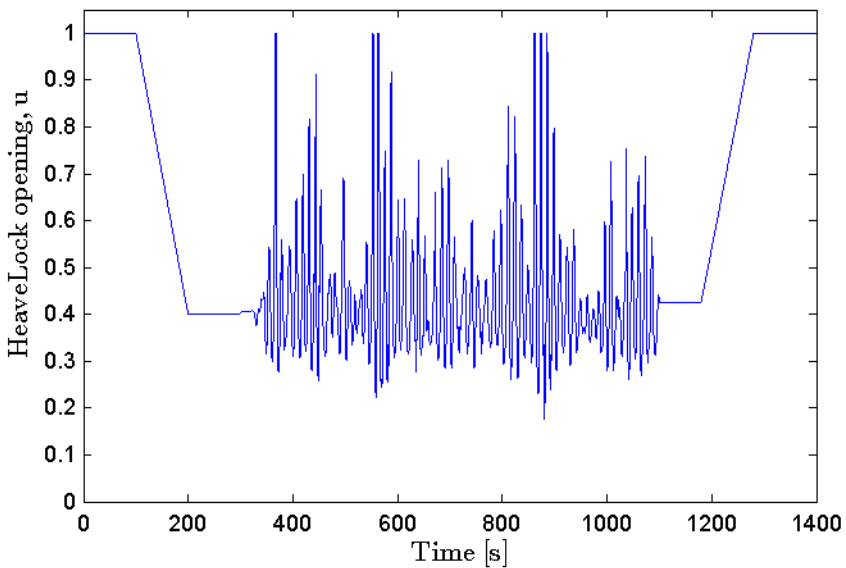


**Figure 6.11:** Case 5b, the HeaveLock opening of the connection simulation, as a function of time, with  $t_{hl}^{buildup} = 100$  s.

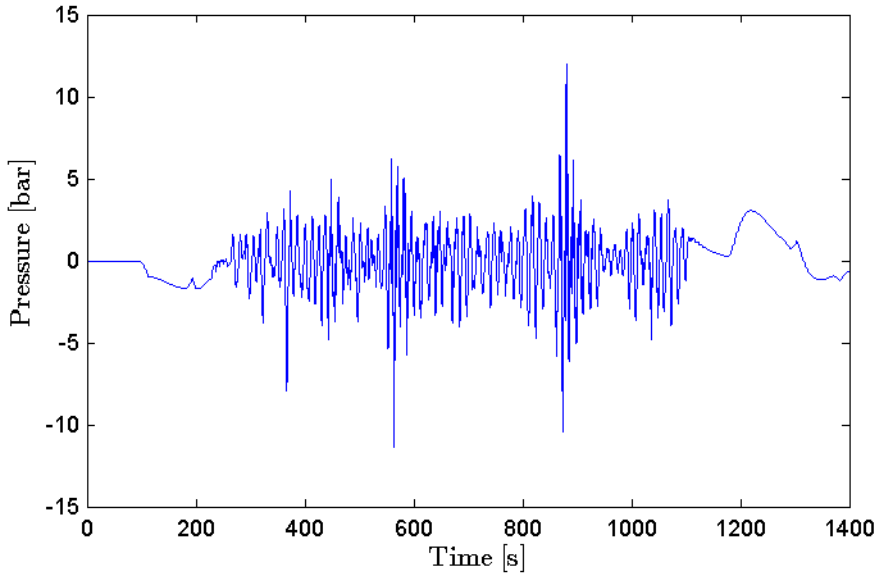


**Figure 6.12:** Case 5b, the downhole pressure difference of the connection simulation, as a function of time, with  $t_{hl}^{buildup} = 100$  s.

### Case 5c, $t_{hl}^{buildup} = 200$ s

For the third case, a long build up interval is chosen;  $t_{hl}^{buildup} = 200$  s. Figures 6.13 and 6.14 show the HeaveLock opening and the downhole pressure of the simulation. The interval the build up is taking place can be seen in Figure 6.13, from  $t = 200$  s to 400 s.

Compared to the two previous simulations, the oscillations in downhole pressure are now of even lower amplitude, around  $\approx \pm 2.2$  bar. Although it is a more satisfying result than for Case 5b, this level of regulating may not be required. If it is not necessary, time could be wasted, using 200 s for this purpose. Again, for use in the real world, requirements on timing and regulation have to be given for each well.

## 6.4 Summary of time parameters

Sections 6.2 and 6.3 both explore time parameters for the initialization (and termination) of the HeaveLock. An acceptable ramping time  $\Delta t_{hl}^1 = \Delta t_{hl}^1$  is found to be about 100 s, giving a pressure peak at both sides of the active period of the HeaveLock at about  $-1.7$  bar and  $3.2$  bar. For the build-up time of the HeaveLock, it is harder to determine what is acceptable, but as there is not a great difference be-

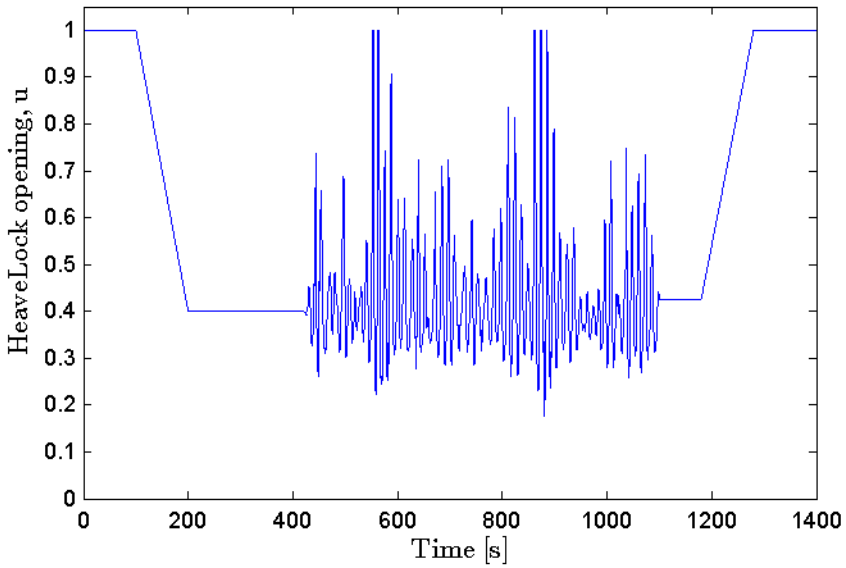


**Figure 6.13:** Case 5c, the HeaveLock opening of the connection simulation, as a function of time, with  $t_{hl}^{buildup} = 200$  s.

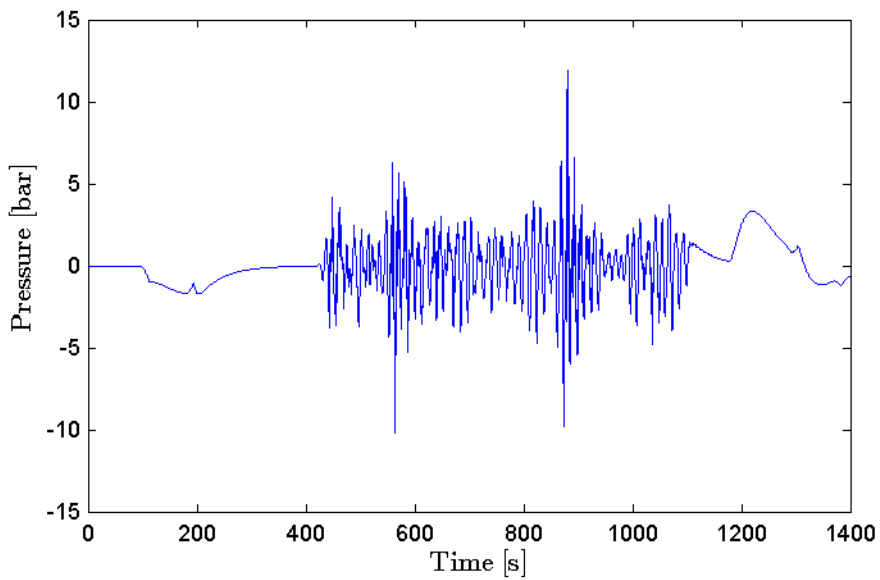


**Figure 6.14:** Case 5c, the downhole pressure difference of the connection simulation, as a function of time, with  $t_{hl}^{buildup} = 200$  s.

tween 100 s and 200 s build up, the build up time chosen for the rest of simulations is 100 s.

## Case 6

From simulations of cases made in this chapter, a resulting case is demonstrated in this section. The resulting alterations can be seen in Figure 6.16, which shows the downhole pressure compared to the same simulation performed without the HeaveLock.

The pressure peak at the end of the simulation reaches 3.2 bar, which is not ideal, as a tentative goal is set at maximum  $\pm 3$  bar. From simulations performed with different ramping times the peak was not improved.

Figure 6.16 compared to Figure 6.6 is not very different. The simulation study performed in this chapter shows that the parameters that are used for the example case in Section 6.1, are close to what is found to yield the best results in the rest of this chapter.

The pump pressure and HeaveLock opening are shown in Figure 6.15. As seen in earlier cases, some saturation in the HeaveLock opening causes the pump pressure to drift a little. This is not ideal, but as the case is simulated for a  $\approx 850$  s connection, and does not effect the pump pressure much, it is not considered fatal.

All time used for initialization and termination add 380 s, or 6 min 20 s, to the HeaveLock connection. For a short connection of 2 – 3 min, this is a considerable amount of time. However, it is needed to complete a connection as successful as the in Figure 6.16.

## 6.5 A tighter simulation

In Section 5.1, cases 1a, b and c demonstrate the effect of changing the nominal HeaveLock opening  $u_0$  for an active sequence of the HeaveLock. It is shown there, how a lower  $u_0$  gave a more well-regulated downhole pressure at the cost of a higher pump pressure.

In the current chapter, all cases run so far have been run with the nominal HeaveLock opening  $u_0 = 0.4$ , and in this section, a case is simulated to show how the performance of a connection is affected by a lowering of nominal HeaveLock opening.

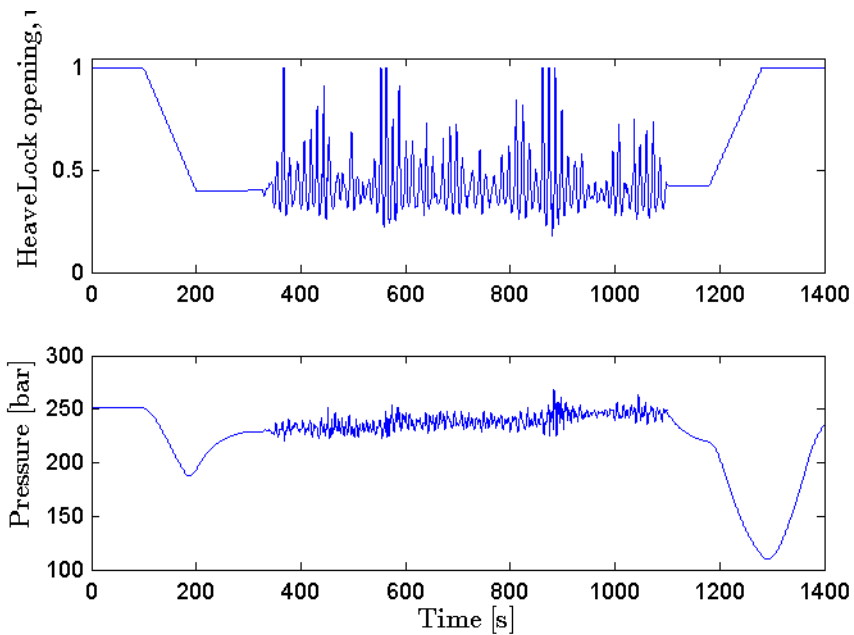


**Figure 6.15:** Case 6, a summary of the time parameters. The figure shows the HeaveLock opening and pump pressure, both as functions of time, of the simulation.

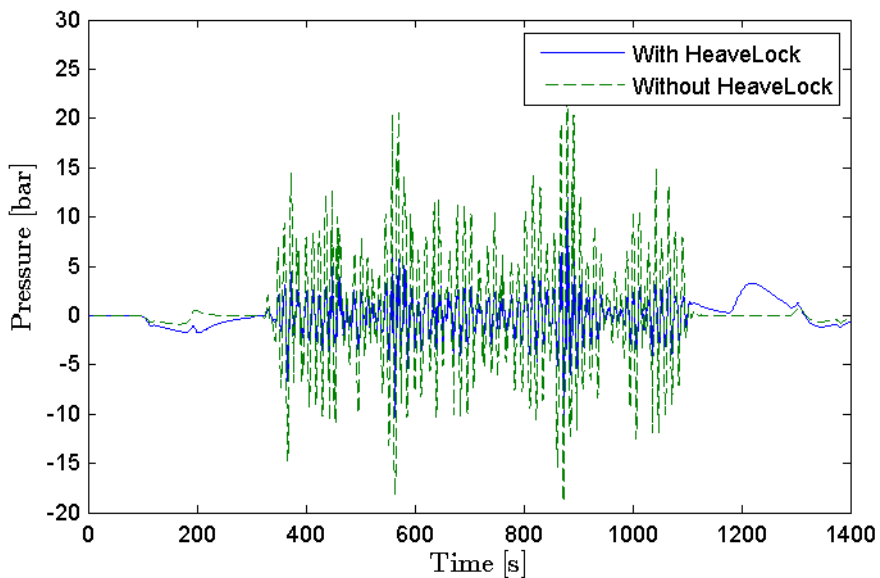


**Figure 6.16:** Case 6, a summary of the time parameters. The figure shows the downhole pressure difference of the simulation compared to the same case without the use of the HeaveLock, as functions of time.

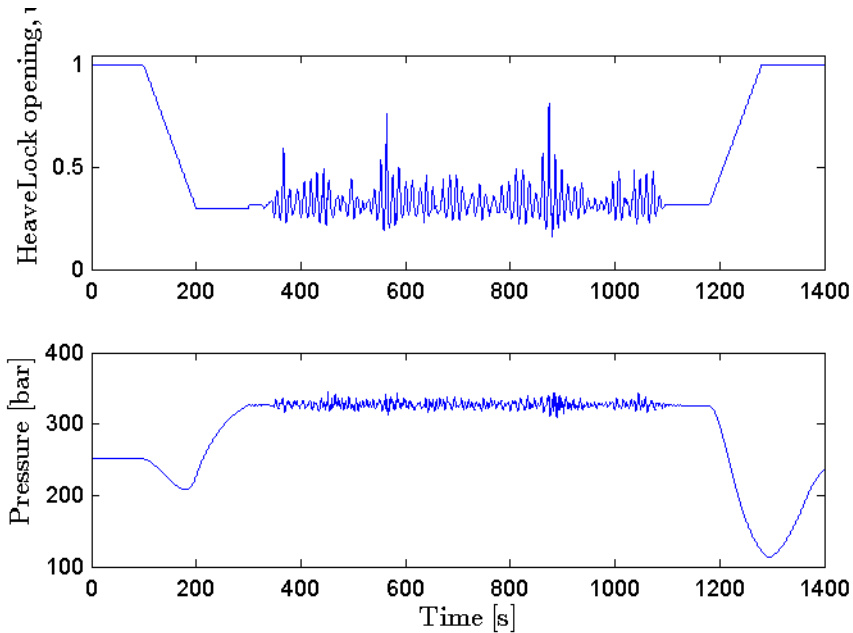


**Figure 6.17:** Case 7, demonstrating the effect of lowering the nominal HeaveLock opening for a connection. The figure shows the HeaveLock opening and pump pressure of the simulation, as functions of time.

### Case 7 - $u_0 = 0.3$

As shown in chapter 5, a lower nominal HeaveLock opening gives better control of the downhole pressure. Case 7 is simulated with the same conditions as for Case 6, except for the altering of the nominal HeaveLock opening from  $u_0 = 0.4$  to  $u_0 = 0.3$ .

Figure 6.17 shows the HeaveLock opening and pump pressure of the Case 7 simulation. During the HeaveLock's active period,  $t = 380$  s to  $t = 1100$  s, the pump pressure is higher than in Figure 6.15, around 330 bar, however still manageable.

The downhole pressure difference in Figure 6.18 is compared to the downhole pressure of the operation without the use of the HeaveLock. The pressure oscillations are lower for Case 7, with the largest peaks of Case 6 also reduced. The pressure waves due to HeaveLock ramping, however, are worsened and are now at  $\approx -3.8$  bar and  $\approx 6$  bar.

This shows that for an initialization of the HeaveLock, the nominal HeaveLock opening can not be altered uncritically, as it has unwanted effects.

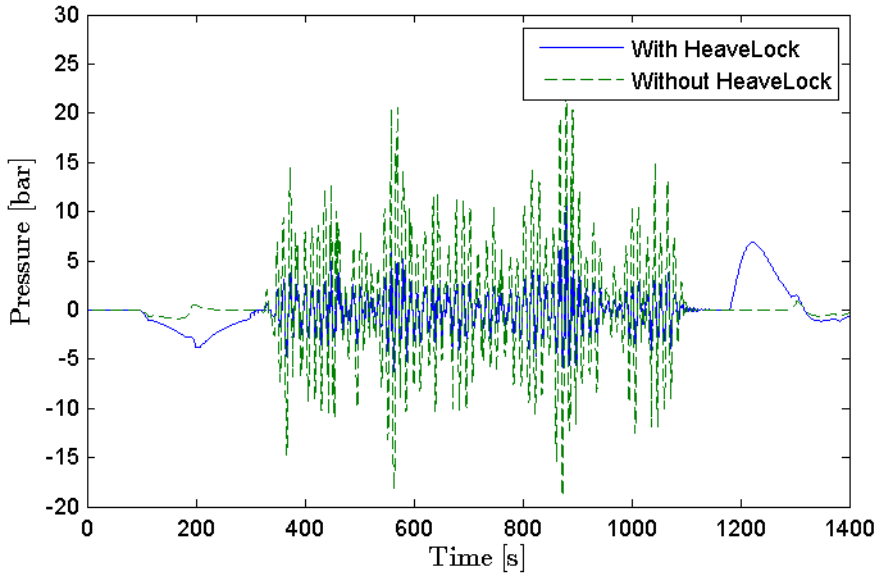


**Figure 6.18:** Case 7, demonstrating the effect of lowering the nominal HeaveLock opening for a connection. The figure shows the downhole pressure difference of the simulation compared to the same case without the use of HeaveLock, as functions of time.

## 6.6 A Short connection

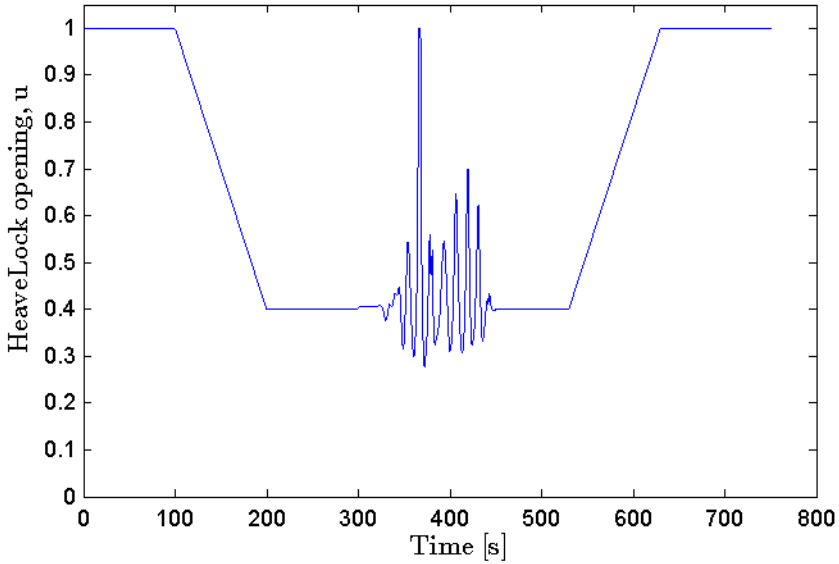
As the last case, it is interesting to check the HeaveLocks performance for a shorter connection time. So far, the simulated connections have been of lengths of about 800–900 s which is, as mentioned in Section 4.4, a long connection. In this section, a more rapid connection simulation of 150 s, or 2.5 min is simulated to investigate whether results from above sections can be transferred.

### Case 8, 150s simulation

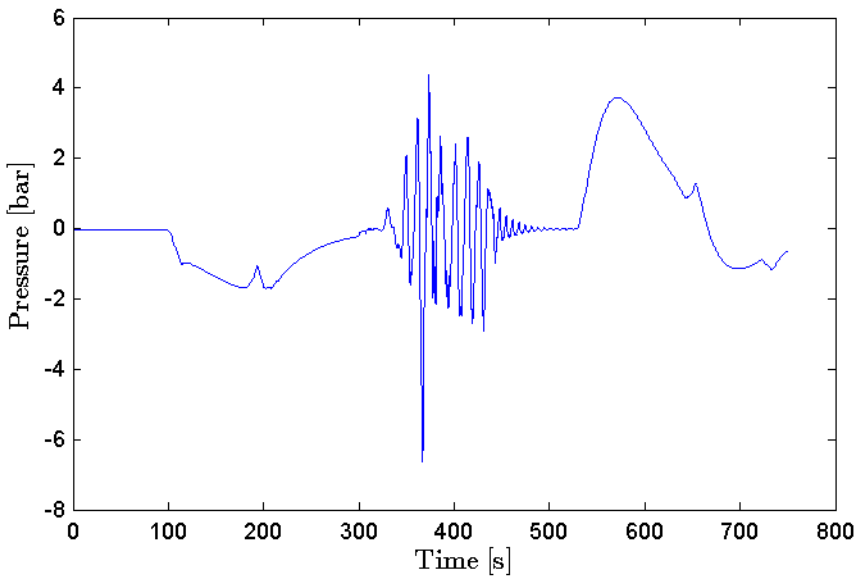
Case 8 is simulated using the same conditions as for Case 7, except for the shortening of the connection itself (the time interval the HeaveLock is active).

Figure 6.20 shows the downhole pressure of the 2.5 min simulation. As the connection time is shorter, it is a little harder to make out whether the pressure is regulated to a satisfactory standard, however, comparing it to the oscillations in Figure 6.18, it seems at though the performance of the regulator is equal as for Case 7.

The pressure peak at the end of the connection, however, reaches  $\approx 3.7$  bar, while for Case 6, the 15 min case, the corresponding peak is 3.2 bar.



**Figure 6.19:** Case 8, showing the HeaveLock opening of the 2.5 min connection simulation, as a function of time.



**Figure 6.20:** Case 8, showing the downhole pressure difference of the 2.5 min connection simulation, as a function of time.



## CHAPTER 7

---

### Discussion

---

When increasing the well depth of the simulation, the result is not affected as much as expected. This may be due to the balancing of the pipe encountering more friction for a deeper well, dampening the movement of the drillstring, versus the time delay that is more dominant the deeper the well gets.

A higher flow rate does, in fact, improve the regulation of pressure surge and swab in the downhole section, however, similar to the well depth, it is not an easily changed parameter, and is rather a condition to work around. The case of flow rate  $2500 \frac{1}{\text{min}}$  and well depth 4000s is the basis for the real world simulations performed in this thesis, and these factors are not tuning parameters for regulation.

Altering the HeaveLock opening is also investigated; in Chapter 5, Case 1 shows that while a lower nominal HeaveLock opening,  $u_0$ , dramatically improves simulations, the potential of this is not limitless as the system, and the pump, in particular, can only bear a certain pressure level.

In Chapter 6, an altering of nominal HeaveLock opening is tested for in a connection in Case 7. It can be seen there that even though the change betters the regulation of downhole pressure during the HeaveLocks active period, it worsens pressure peaks due to ramping of the HeaveLock. To keep these disturbances at an acceptable level,  $u_0$  can not be changed freely, and this could make the requested level of attenuation unattainable.

As seen in many cases in both Chapters 5 and 6, saturation of the HeaveLock leads to drift in pump pressure. For a poorly regulated sequence of the active HeaveLock, this could prove fatal, but two factors speak to the fact that this will

not be a problem. First, most of the connections simulated in Chapter 6 are considered long simulation, and even for some saturation of the HeaveLock, the pump pressure does not drift more than 30 bar for the entire period. Second, the HeaveLock should not saturate much, as this leads to poor regulation of the downhole pressure.

The effect of increasing the time interval for ramping the HeaveLock opening, demonstrated in cases 4a, b and c, is that it decreases its effect on the downhole pressure. However, from the simulation study, the disturbances due to termination ramping are only dampened to 3.2 bar (Case 6) and 3.7 bar (Case 8), which is higher than the tentative goal, set at 3 bar.

When initialized, the HeaveLock's opening is held at the nominal HeaveLock opening for a certain time period. Three different interval times are tested for in cases 5a, b and c. Increasing this build-up time can improve the downhole pressure regulation somewhat, while not affecting ramping disturbance. However, this also adds time to the connection, and so the interval should still be kept at a reasonable time period.

If progress could be made on the HeaveLock regulator, and better control of the heave motion could be attained for a larger nominal HeaveLock opening than what is currently possible, it could be concluded that the HeaveLock had even more promise, as the ramping disturbances currently increase for a smaller nominal HeaveLock opening. However, with a connection procedure (shown in cases 6 and 8), the HeaveLock still managed to attenuate about 70% of the pressure oscillations in the downhole section, with a ramping disturbance at maximum 3.2 and 3.7 bar.

Another issue of the RealPlant simulator is that it assumes zero time delay in changing the HeaveLock opening. For a deep well, the time delay, in reality, could be a significant factor.

The simulations in this thesis have been run for a set of dimensions and physical factors, based on reasonable assumptions. For the simulation of the HeaveLock for a given well, the simulator dimensions and physical factors would have to be re-entered to give a realistic impression on how the HeaveLock would act for that specific instance.

## CHAPTER 8

---

### Conclusion

---

For a given well, the HeaveLock will dampen downhole pressure oscillations due to rig heave to almost any level. The HeaveLock's nominal opening can be lowered, to better the regulation in the time interval of the connection itself, bettering the regulation of downhole pressure during the HeaveLocks active period.

Lowering the HeaveLock opening, however, worsen pressure peaks due to ramping of the HeaveLock and increases the pump rate. A low pump pressure is favoured for more than one reason; it lowers the power needed to operate, and it also reduces the wear on the system, as well as the chance of leaks, giving economic and environmental advantages.

To keep disturbances due to initialization and termination of the HeaveLocks function at an acceptable level and the same time ensure a realizable pump pressure level,  $u_0$  can not be changed freely. This restraint could make the requested level of attenuation unattainable.

Increasing the time of ramping the HeaveLock opening down or up does better downhole pressure disturbance, but at the cost of more time added to the connection. Lengthening the time interval the HeaveLock has to build up back pressure before it is activated can also improve regulation without affecting the ramping disturbances, again at the penalty of more time added to the connection. For a given well, either regulation or timing requirements have to be set to decide whether these intervals can be increased or decreased.

If the regulation of the HeaveLock could be improved so that the initialization and termination of it could be unaffected by the change in nominal opening somehow,

even better regulation of the downhole pressure could be achieved. This thesis, however, shows that the HeaveLock regulator and its initialization and termination needs further investigations.

## 8.1 Further work

As this thesis does not go into depth in gathering information on the conventional heave attenuation method that would be used outside the connection, the termination and initialization need looking into. Can the conventional method be connected and disconnected as needed? Can initializing and terminating the conditions needed for the HeaveLock be done while the conventional attenuation method is active?

As mentioned, the HeaveLocks choke characteristic is assumed linear, but is not the case in reality. Because of this, there will be a limit to how 'good' the regulation will be, and especially how well it can relate to reality.

Eventually, bettering the HeaveLock regulator in the simulator will have the potential to provide valuable knowledge of the actuator in a real oil well, and this bears the promise to achieve more realistic heave attenuation in the long term.

A problem in doing connections has in this thesis been proven to be pressure disturbance when ramping the HeaveLock opening up and down. An interesting possibility to better this issue could be to apply optimization techniques on ramping procedures of flow, topside choke and HeaveLock, to explore the potential of the lowest possible disturbance when initializing and terminating.

After completing optimization of initialization and termination, the potential of how low these disturbances can get can be uncovered. If ramping can be done more safely, it would give more space to alter the nominal HeaveLock opening  $u_0$  and thereby giving a theoretical way to have tight control without great disturbances from activating and deactivating the HeaveLock.

Optimization techniques might be the way forward in using the existing modeling of the HeaveLock. However, if it is not possible to attenuate ramping disturbances entirely, altering the regulation of the HeaveLock should be the way forward. Even in managing to cancel the ramping disturbances entirely, a low nominal HeaveLock opening still requires an increasing pump pressure, which may not be realizable.

---

## Bibliography

---

- Aarsnes, U. J. F., June 2012. Reduced order observer design for managed pressure drilling. Master's thesis, Norwegian University of Science and Technology.
- Aarsnes, U. J. F., Aamo, O. M., Pavlov, A., 2012. Quantifying error introduced by finite order discretization of a hydraulic well model.
- Aarsnes, U. J. F., Gleditsch, M. S., Aamo, O. M., Pavlov, A., 2014. Modeling and avoidance of heave-induced resonances in offshore drilling. *SPE Drilling & Completion* 29 (04), 454–464.
- Albert, A., June 2013. Disturbance attenuation in managed pressure drilling. Master's thesis, Norwegian University of Science and Technology.
- Albert, A., Aamo, O. M., Godhavn, J.-M., Pavlov, A., 2014. Suppressing pressure oscillations in offshore drilling: Control design and experimental results. *IEEE TRANSACTIONS ON CONTROL SYSTEMS TECHNOLOGY* 23 (2), 813–819.
- Birkeland, T., June 2009. Automated well control using mpd approach. Master's thesis, University of Stavanger.
- GardenDenver, 2016. Pz 11hp (pzl hp) pump model.  
URL <http://www.gardnerdenverpumps.com/pumps/drilling/pz11hp/>
- Godhavn, J.-M., Pavlov, A., Kaasa, G.-O., Rolland, N. L., 2011. Drilling seeking automatic control solutions. 18th IFAC World Congress.
- Guardian, T., December 2015. Recession, retrenchment, revolution? impact of low crude prices on oil powers.  
URL <http://www.theguardian.com/business/2015/dec/30/oil-iran-saudi-arabia-russia-venezuela-nigeria-libya>

- 
- IADC, 2008. Underbalanced operations and managed pressure drilling glossary. International Association of Drilling Contractors (IADC).
- International Association of Geophysical Contractors, I., 2014. Environmental benefits of seismic surveys.  
URL <http://www.iagc.org/>
- Jenner, J. W., Elkins, H., Springett, F., Lurie, P., Wellings, J. S., 2005. The continuous-circulation system: An advance in constant-pressure drilling. SPE Drilling & Completion 20 (03), 168–178.
- Kaasa, G.-O., 2000. A simple dynamic model of drilling for control.
- Kaasa, G.-O., Imsland, L., Pavlov, A., 2010. Experimental disturbance rejection on a full-scale drilling rig. 8th IFAC Symposium on Nonlinear Control Systems.
- Landet, I. S., June 2011. Modeling and control for managed pressure drilling from floaters. Master’s thesis, Norwegian University of Science and Technology.
- Mitchell, R. F., 1988. Dynamic surge/swab pressure predictions. SPE Drilling Engineering 3 (03), 325–333.
- PU, P. U., October 2015. Cylinder stress.  
URL [http://www.tech.plym.ac.uk/sme/MECH115-web/Cylinders%20&%20Spheres\(8\).PDF](http://www.tech.plym.ac.uk/sme/MECH115-web/Cylinders%20&%20Spheres(8).PDF)
- Schaut, S., September 2015. Modeling, estimation and control for an experimental lab facility for drilling. Master’s thesis, Norwegian University of Science and Technology.
- Schlumberger, 2016. Oilfield glossary.  
URL <http://www.glossary.oilfield.slb.com/>
- Øyvind Breyholtz, Nygaard, G., Godhavn, J.-M., Vefring, E. H., 2009. Evaluating control designs for co-ordinating pump rates and choke valve during managed pressure drilling operations. 18th IEEE International Conference on Control Applications.

---

# Appendix

## Appendix A: The RealPlant Simulator

The RealPlant simulator used in this thesis is in a separate zip-file.

To run RealPlant, make a new matlab script file in the RealPlant folder. The following code will run two cases, one using the HeaveLock and one not using the HeaveLock for the same sequence of disturbance:

```
clear all
% close all
clc

addpath('data')
%% Defining preliminary parameters
dt = 0.1;
t0 = 0;
t1 = 1400;
t = t0:dt:t1;

heavelock_pos = 1;% HeaveLock position

%% Defining heave motion using measured heave data
fileID = fopen('/data/Heave1.txt');
C = textscan(fileID, '%s %s %f');
fclose(fileID);
heave_data_x = C{3}(2:end);
heave_data_v = [heave_data_x(2)-heave_data_x(1); ...
    (heave_data_x(3:end) - heave_data_x(1:end-2))/2; ...
    heave_data_x(end)-heave_data_x(end-1)];
L = length(heave_data_v);
v_rig = @(t) interp1(0:L-1,heave_data_v(1:L),t);

% Smoothing initial trajectory
offset_width = 10;
offset = @(x) (x>offset_width);
smoothing_width=30;
smoothstep = @(x) ((x-offset_width).^2.*(3/smoothing_width^2-2/...
    smoothing_width^3*(x-offset_width)).*(x<=smoothing_width+...
    offset_width) + (x>smoothing_width+offset_width);
v_rig = @(t) v_rig(t).*smoothstep(t).*offset(t);
v_rig_scaled = @(t) 2*v_rig(t);
```

---

```
% HeaveLock parameters
t_switch = offset_width;
p_hl_drop = 50*1e5;
u_min = 0.05;

%% Simulation
q_pump = [2500];          % pump flow [l/min]
q_pump = q_pump/(1000*60); % pump flow [m^3/s]
well_length = [4000];    % well length [m]

params = def_params(q_pump,well_length,u0,p_hl_drop,u_min,t_switch);
model = def_model(params,v_rig_scaled,heavelock_pos, false);
model_hl = def_model(params,v_rig_scaled,heavelock_pos, true);

[t_sim,x] = model.simulate(t);
[t_hl,x_hl] = model_hl.simulate(t);
```